Ann. Naturhist. Mus. Wien	110 A	345–381	Wien, Jänner 2009

The Jurassic-Cretaceous boundary in the Gresten Klippenbelt (Nutzhof, Lower Austria): Implications for Micro- and Nannofacies analysis

Daniela REHÁKOVÁ[1], Eva HALÁSOVÁ[1], Alexander LUKENEDER[2]

(With 6 plates and 4 figures)

Manuscript submitted on September 11th 2008,
the revised manuscript on November 3rd 2008.

Abstract

The paper discusses the results of an integrated study of three microplankton groups (calpionellids, calcareous dinoflagellates and nannofossils) and macrofauna (ammonites, belemnites and aptychi) in the Nutzhof section. The stratigraphic investigation of the microfauna revealed that Nutzhof comprises a sedimentary sequence of Early Tithonian to Middle Berriasian age. Based on the distribution of the stratigraphically important planktonic organisms, several coeval calpionellid, dinocyst and nannofossil bioevents were recorded along the Jurassic-Cretaceous boundary beds.

Keywords: Calcareous microfossils, Nannofossils, Pelagic carbonates, J/K boundary, Gresten Klippenbelt.

Zusammenfassung

Der Artikel diskutiert die Ergebnisse einer ganzheitlichen Studie von drei Mikroplankton Gruppen (Calpionellen, kalkigen Dinoflagellaten und Nannofossilien) und der Makrofauna (Ammoniten, Belemniten und Aptychen) an der Sektion Nutzhof. Die stratigrafischen Untersuchungen der Mikrofauna erbrachten für die sedimentäre Sequenz von Nutzhof ein Alter von unterem Tithonium bis mittlerem Berriasium. Basierend auf der Verbreitung von stratigrafisch wichtigen planktonischen Organismen, konnten einige gleichaltrige Calpionellen-, Dinozysten- und Nannofossil-Events um die Jura-Kreide Grenz Schichten nachgewiesen werden.

Schlüsselworte: Kalkige Mikrofossilien, Nannofossilien, Pelagische Karbonate, J/K Grenze, Grestener Klippenzone.

1. Introduction to the geology and lithology of the Nutzhof section

This study presents the results of a joint geophysical and palaeontological project focused on detailed palaeontological studies around the Jurassic-Cretaceous (J/K) boundary. The Nutzhof section is situated in the Gresten Klippenbelt at Nutzhof (Lower Austria) (Fig.

[1] Department of Geology and Palaeontology, Faculty of Natural Sciences, Comenius University, Mlynská dolina G-1, 842 15 Bratislava, Slovakia; e-mail: rehakova@fns.uniba.sk; halasova@fns.uniba.sk

[2] Natural History Museum Vienna, Geological-Palaeontological Department, Burgring 7, 1010 Vienna, Austria; e-mail: alexander.lukeneder@nhm-wien.ac.at

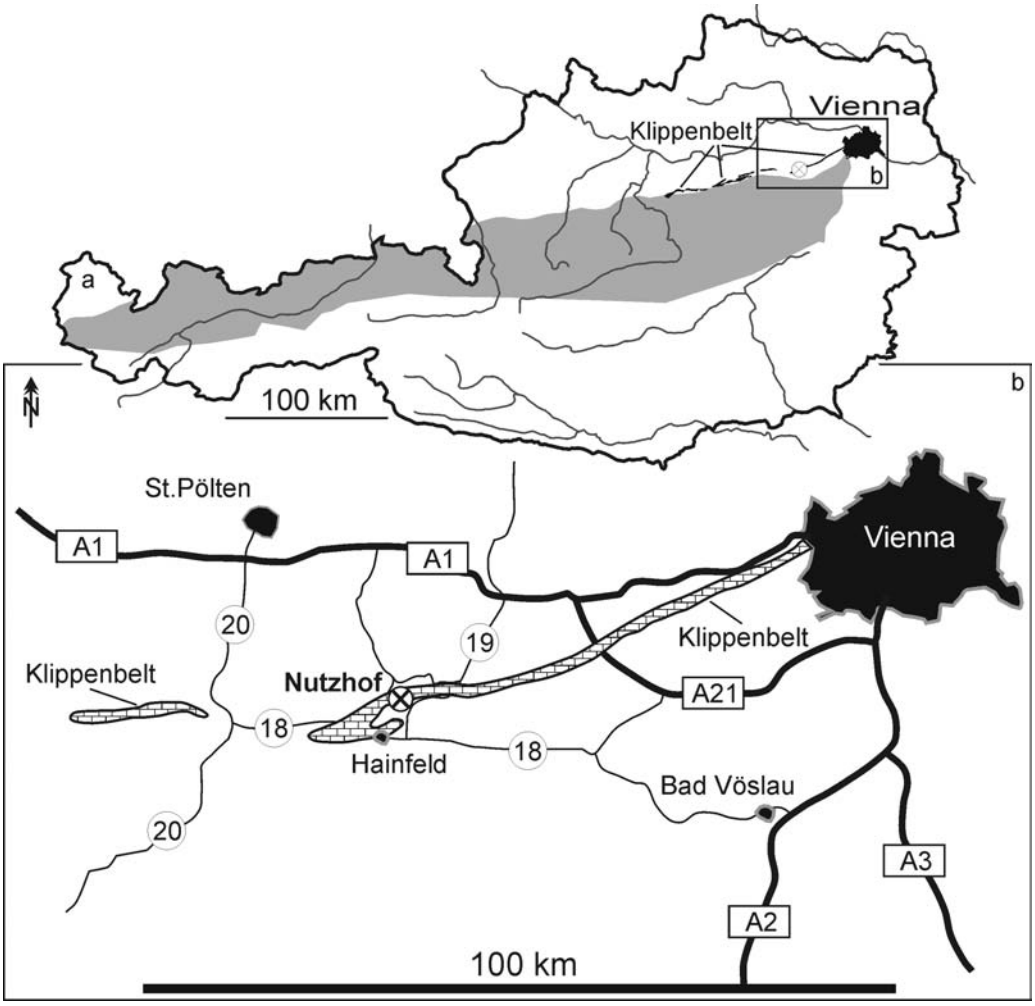

Fig. 1: Geological situation and localization of the Nutzhof section in Lower Austria from LUKENEDER (2009; this volume).

1). It yields a record of pelagic marine sedimentation in the Austrian Gresten Klippenbelt, located in the southern Flysch Zone. The first study of the lithology and stratigraphy of this area was provided by CŽIŽEK (1852), followed later by KÜPPER (1962). For a more detailed description of the Nutzhof section see LUKENEDER (this volume).

The preliminary results of micro- and nannofacies analysis and magnetostratigraphic investigations of the limestone sequence in the Nutzhof section were published by REHÁKOVÁ et al. (2009) and PRUNER et al. (2009). The data presented in this paper show that the Jurassic-Cretaceous pelagic limestone sequence of the Nutzhof section offers the possibility to clearly document the J/K boundary interval in the Austrian Gresten Klippenbelt based solely on the good calpionellid, dinoflagellate and nannofossil stratigraphic record.

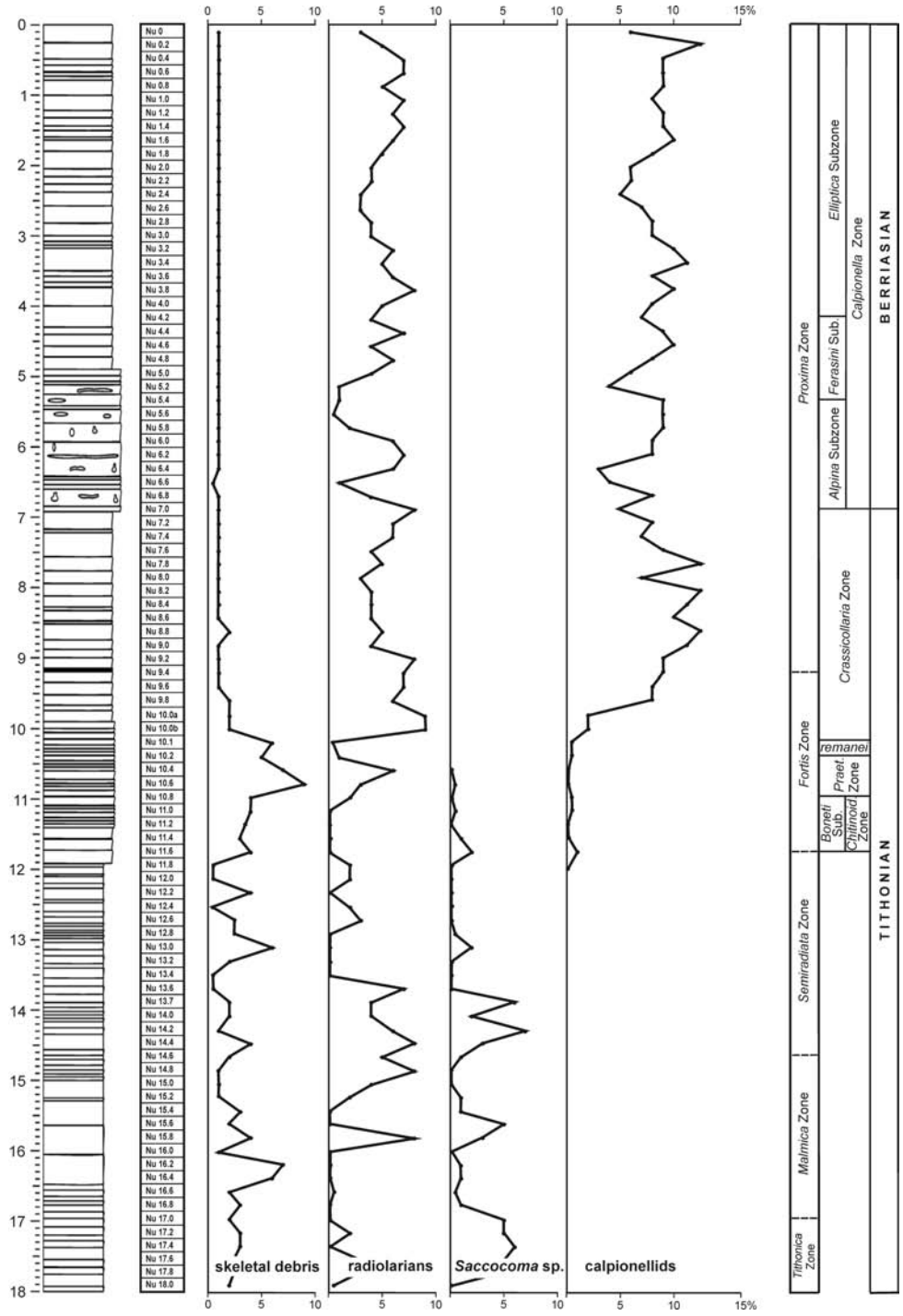

Fig. 2: Age, lithology and quantitative abundance of selected groups of organisms of the Nutzhof section.

2. Material and methods

The Jurassic-Cretaceous boundary sequence of the Nutzhof section was studied using an integrated biostratigraphy approach on the detailed rock section sampled. A quantitative microfacies analysis involved a thin sections study (fig. 2). Sample numbers, for example Nu 10.0, correspond to the sample interval at 10.0 meter within the log (for all numbers and figures, Nu Nutzhof). The calpionellids and calcareous dinoflagellates were studied under a light microscope LEICA DM 2500 P in 93 thin sections and they were documented by camera LEICA DFC 290 HD in Bratislava. Thin sections are deposited in the archive of the Natural History Museum in Wien (NHMW 2008z0271/0001-0036). Changes in the distribution of these organism remnants (fig. 3) in the microfacies were studied in detail in order to correlate them with the changes in nannoplankton associations (fig. 4).

Calcareous nannofossils were analyzed semiquantitatively in 19 smear slides prepared from all lithologies by standard techniques. The study was carried out using a light polarizing microscope at 1250x magnification. In order to obtain relative abundances, at least 200 specimens were counted in each slide. Their vertical distributions were recorded (fig. 4). Nannofossil preservation can be characterized as moderately to heavily etched by dissolution. Our study follows the zonal scheme proposed by BRALOWER et al. (1989).

A total of 46 ammonite specimens and 238 lamellaptychi were examined (LUKENEDER this volume). Four brachiopods and 3 inoceramids, along with single belemnite specimen, were collected. Ammonites are preserved (moderately well) as steinkerns. No shell is present. The phramocones are mostly flattened, whereas the body chambers are better preserved because of their history of early sediment infilling. The fragmentation is due to preburial-transport, sediment compaction and considerable tectonic deformation. This complicates the precise determination of most cephalopods with chambered hardparts (e.g. ammonites and belemnites). Most of the ammonite specimens were collected using hammers. The specimens required preparation with vibration tools after having been washed.

3. Results

3.1. Microfacies analysis – calpionellid and dinoflagellate biostratigraphy

The studied limestones are wackestones, packstones or mudstones. The observed fine-grained micrite with pelagic microfossils (calpionellids, calcareous dinoflagellates, radiolarians and calcareous nannofossils) is common in open-marine environments. The rare skeletal debris derived from fragmented and disintegrated shells of invertebrates (benthic foraminifers, echinoderms, molluscs) come from shallower environments. The studied microfacies are typical for basinal settings, which could also be situated in tectonically influenced, subsiding shelf areas.

The distribution, abundance and diversity of calcareous dinoflagellate cysts are important from both the stratigraphic and palaeoenvironmental points of view. We followed the calcareous dinoflagellate cyst zonation sensu REHÁKOVÁ (2000b). The preservation of the calpionellids is generally good. Their quantitative representation is variable, from

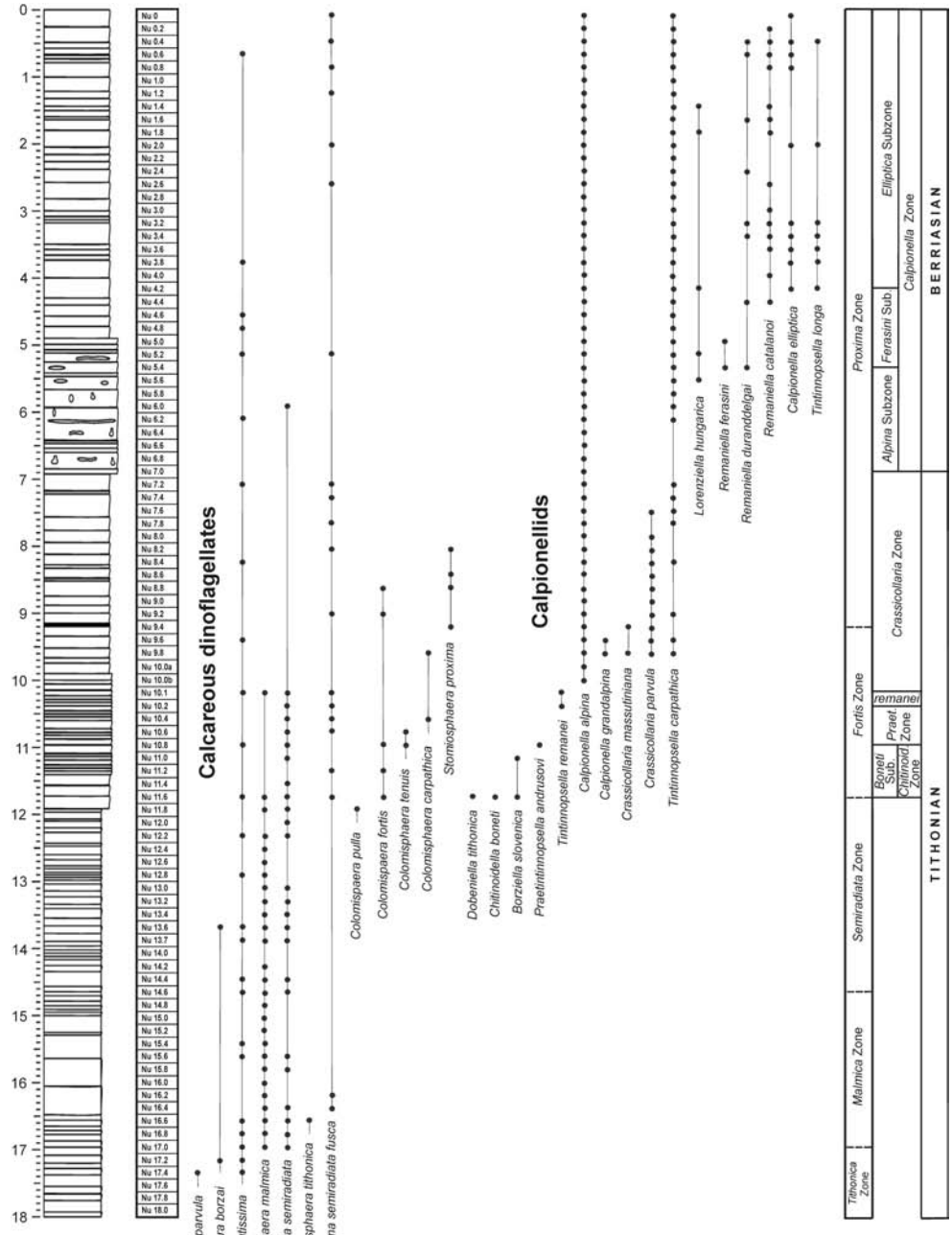

Fig. 3: Age, lithology, calpionellid and calcareous dinoflagellate biostratigraphy and vertical distribution of the recorded calpionellid and dinoflagellate species of the Nutzhof section.

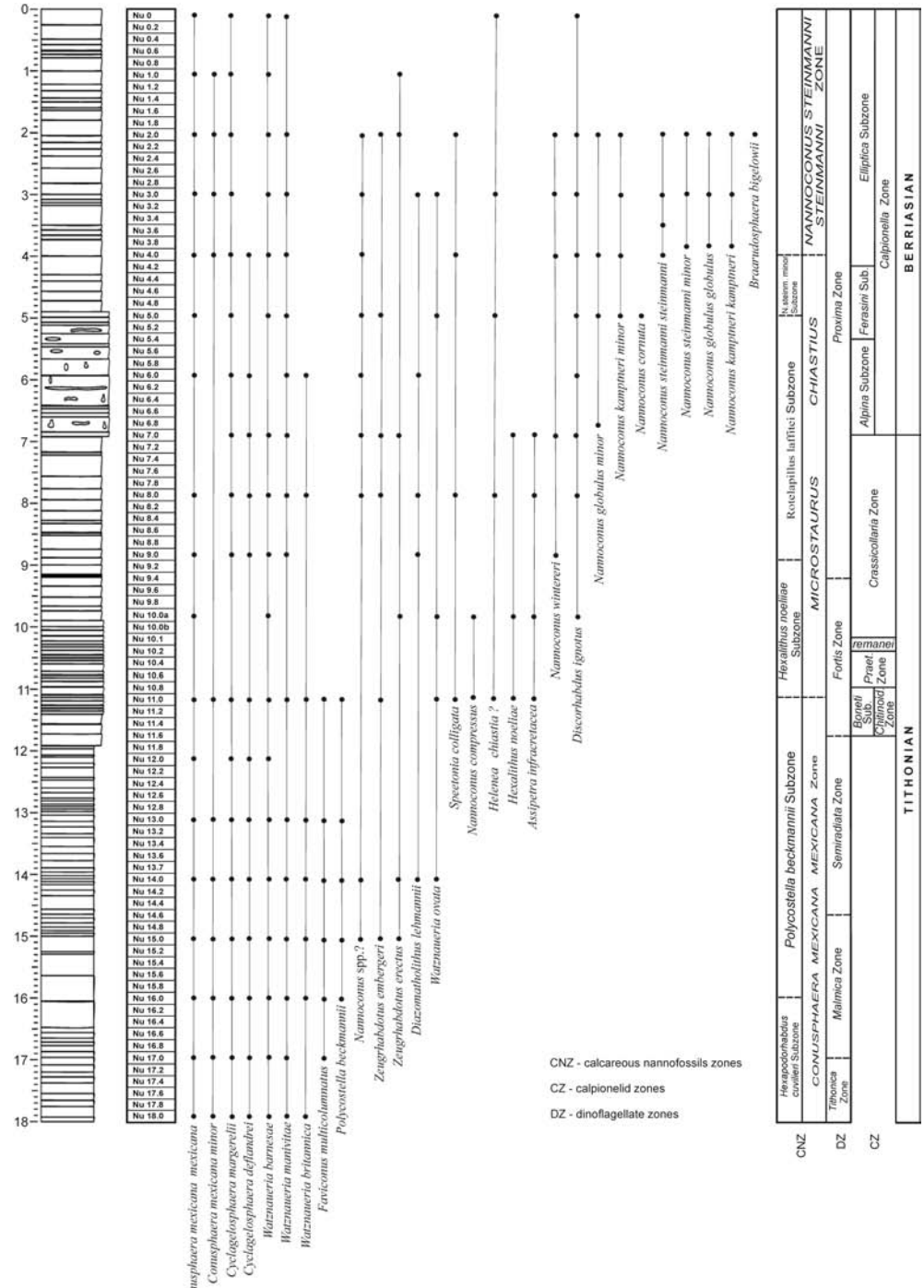

Fig. 4: Age, lithology, nannofossil biostratigraphy and vertical distribution of nannofossil species of the Nutzhof section.

less frequent in the case of chitinoidellids to more abundant in the hyaline forms of calpionellids. Although the chitinoidellids are not perfectly preserved, they enabled the application of POP´s (1997) and REHÁKOVÁ´s (2002) taxonomy. This study allows the *Boneti* Subzone to be recognized in the frame of the *Chitinoidella* Zone. The standard calpionellid zones and subzones, as proposed by REHÁKOVÁ (1995) and REHÁKOVÁ & MICHALÍK (1997), were adopted.

The following dinoflagellate and calpionellid associations and zones were recognized in the Nutzhof section (fig. 3).

***Tithonica* Zone** (the interval limited by samples 18.0 – 17.2)

It is represented by bioturbated biomicrite limestones (mudstones) with variable abundance of skeletal debris. Limestones contain calcified radiolarians (locally pyritized), sponge spicules, aptychi, ostracod and crinoid fragments, rare *Saccocoma* sp., *Cadosina parvula* NAGY, *Schizosphaerella minutissima* (COLOM), *Carpistomiosphaera borzai* (NAGY; pl. 1, fig.1) and *Carpistomiosphaera tithonica* NOWAK. Skeletal fragments are concentrated in nests and irregular fine-grained laminae or in tiny layers often rich in Fe-hydroxides. The matrix is stylolitized; locally, many composed stylolites and also thin calcite veins penetrate the biomicrite mudstones. Silty glauconite is also visible. **Early Tithonian.**

***Malmica* Zone** (the interval limited by samples 17.0 – 14.8)

The layers are built by bioturbated mudstones with rare biofragments dispersed in the matrix (pl. III. figs. 1, 2): bivalves, ostracods, ophiurid and rycholite fragments (pl. 4, fig. 1), calcified radiolarians, sponge spicules, *Dentalina* sp., *Spirilina* sp., *Saccocoma* sp., *Parastomiosphaera malmica* (BORZA; pl. 1, fig. 2), *Cadosina semiradiata semiradiata* WANNER (pl. 1, fig. 3), *Cadosina semiradiata fusca* (WANNER), *Carpistomiosphaera tithonica* NOWAK and *Schizosphaerella minutissima* (COLOM). The matrix is penetrated by thin calcite veins. Thin laminae composed of fine-grained silt with muscovite and clay minerals and matrix rich in stylolites, framboidal pyrite and glauconite are documented in several thin sections. Pyrite is usually concentrated into the nests (pl. 3, fig. 3). Locally, the marly matrix has a pelitic structure. In this case the content of biofragments is very low – (thin sections contain very rare *Parastomiosphaera malmica* (BORZA) and silty glauconite). The last sample of this interval shows a distinct gradation of biodetritus. **Early Tithonian.**

***Semiradiata* Zone** (samples 14.6 – 11.8)

Marly limestones – biomicrite mudstones often bioturbated, containing aptychi, ostracods, crinoids, juvenile ammonite, bivalves, sponge spicules, calcified radiolarians concentrated in nests, *Saccocoma* sp., dinocysts: *Parastomiosphaera malmica* (BORZA), *Colomisphaera pulla* (BORZA; pl. 1, fig. 4), *Cadosina semiradiata semiradiata* WANNER and *Schizosphaerella minutissima* (COLOM). Biofragments are impregnated by Fe oxides/hydroxides (pl. 3, fig. 4). Locally, the matrix is penetrated by abundant calcite veins; it also contains framboidal pyrite and silty glauconite. The matrix in sample 13.4 reveals the marks of synsedimentary deformation (pl. 4, fig. 2), sample 13.2 contains thin layers (or laminae) rich in biodetritus. The matrix has a micropelitic structure locally. **Early Tithonian–Middle Tithonian**.

***Chitinoidella* Zone** (samples 11.6 – 11.0)

Biomicrite limestones – mudstones with input of skeletal debris concentrated in thin laminae (pl. III. fig. 5). They contain aptychi, bivalves, ostracods (locally also with ornamented shells), crinoids, ophiurids, sponge spicules, *Saccocoma* sp., *Colomisphaera fortis* ŘEHÁNEK (pl. 1, figs. 5-6), *Parastomiosphaera malmica* (BORZA), *Schizosphaerella minutissima* (COLOM), *Cadosina semiradiata semiradiata* WANNER. The calpionellid assemblage is characterized by: *Borziella slovenica* (BORZA; pl. 2, fig. 1), *Dobeniella tithonica* (BORZA) and *Chitinoidella boneti* DOBEN (pl. 2, fig. 2). Part of the thin section (sample 11.6) rich in biodetritus is limited by the thin clay laminae and slowly passes to micrite limestone, which is penetrated by abundant calcite veins. Besides a fine clay admixture, the samples also contain glauconite, locally accumulations of pyrite cubes or framboidal pyrite (pl. 3, fig. 6). **Middle Tithonian.**

***Praetintinnopsella* Zone** (samples 10.8 – 10.4)

Bioturbated mudstones with laminae of fine detritus (pl. 4, figs. 3, 4). The studied samples contain radiolarians, ostracods, crinoids, sponge spicules, bivalves, foraminifers, *Cadosina semiradiata semiradiata* WANNER, *Schizosphaerella minutissima* (COLOM), *Colomisphaera fortis* ŘEHÁNEK, *Colomisphaera carpathica* (Borza), *Colomisphaera tenuis* (NAGY; pl. 1, fig. 7), and *Praetintinnopsella andrusovi* BORZA. They also contain a small portion of glauconite and pyrite (locally nests of framboidal pyrite). The matrix in some samples is penetrated by thin calcite veins. Locally, mudstone passes to radiolarian-sponge wackestone with rich accumulation of radiolarians and sponge spicules. **Earliest Late Tithonian**.

***Crassicollaria* Zone, *Remanei* Subzone** (samples 10.2 – 10.1)

Bioturbated mudstone with laminae of fine biodetritus rich in calcareous cysts. It contains radiolarians, sponge spicules, ostracods, *Tintinnopsella remanei* BORZA (pl. 2, fig. 3), *Cadosina semiradiata semiradiata* WANNER, *Schizosphaerella minutissima* (COLOM) and *Parastomiosphaera malmica* (BORZA). The matrix is penetrated by abundant, thin calcite veins. **Late Tithonian**.

***Crassicollaria* Zone**, ***Intermedia* Subzone** (samples 10.0 – 7.2)

Radiolarian-calpionellid or calpionellid-radiolarian wackestones (pl. 4, fig. 5). Wackestones pass locally to radiolarian packstone (mainly in small chert accumulations). The matrix contains aptychi, foraminifers, radiolarians, bivalves, sponge spicules, *Calpionella alpina* LORENZ (loricas are locally coated by dark, microgranular calcite), *Calpionella grandalpina* NAGY (pl. 2, fig. 4), *Crassicollaria massutiniana* (COLOM), *Crassicollaria parvula* REMANE (pl. 2, fig. 5), *Tintinnopsella carpathica* (MURGEANU & FILIPESCU), *Colomisphaera carpathica* (BORZA), *Schizosphaerella minutissima* (COLOM), *Stomiosphaerina proxima* ŘEHÁNEK (pl. 1, fig. 8), *Cadosina semiradiata fusca* (WANNER) and *Colomisphaera fortis* ŘEHÁNEK. The matrix of several samples is penetrated by rich calcite veins of different orientation. They are filled by blocky and fibrous calcite crystals. **Late Tithonian.**

***Calpionella* Zone, *Alpina* Subzone** (samples 7.0 – 5.6)

Calpionellid-radiolarian, radiolarian-calpionellid wackestones, locally calpionellid mudstones or mudstones penetrated by calcite veins (pl. 4, fig. 6). They contain aptychi, bivalves, crinoids, sponges, and radiolarians. In the lower part of the studied interval, a monospecific calpionellid association consisting of *Calpionella alpina* LORENZ is present, being accompanied in the overlying beds by *Tintinnopsella carpathica* (MURGEANU & FILIPESCU), *Lorenziella hungarica* KNAUER, *Stomiosphaerina proxima* ŘEHÁNEK (pl. 1, fig. 9) and *Schizosphaerella minutissima* (COLOM). **Lower Berriasian-J/K boundary**.

***Calpionella* Zone, *Ferasini* Subzone** (samples 5.4 – 4.4)

Radiolarian-calpionellid, calpionellid-radiolarian, locally calpionellid wackestones with calcified radiolarians, crinoids, aptychi, bivalves, ostracods, *Schizosphaerella minutissima*, *Cadosina semiradiata fusca*, *Calpionella alpina* LORENZ, *Tintinnopsella carpathica* (MURGEANU & FILIPESCU), *Remaniella ferasini* (CATALANO), *Remaniella duranddelgai* POP (pl. 2, fig. 6), *Remaniella catalanoi* POP and *Lorenziella hungarica* KNAUER. The matrix is locally penetrated by calcite veins. **Lower Berriasian**.

***Calpionella* Zone, *Elliptica* Subzone** (samples 4.2 – 0.0)

Predominantly radiolarian-calpionellid wackestones with radiolarians, sponge spicules, aptychi, *Punctaptychus*, crinoids, ostracods, bivalves, foraminifers, *Lenticulina* sp., *Schizosphaerella minutissima* (COLOM), *Cadosina semiradiata fusca* (WANNER), *Calpionella alpina* LORENZ, *Tintinnopsella carpathica* (MURGEANU & FILIPESCU), *Tintinnopsella longa* (COLOM; pl. 2, fig. 7), *Remaniella catalanoi* POP (pl. 2, fig. 8), *Remaniella duranddelgai* POP, *Calpionella elliptica* CADISCH (pl. 2, fig. 9) and *Lorenziella hungarica* KNAUER (part of loricas have dark coats). Locally, the matrix contains dispersed pyrite; moreover, part of the organic fragments is impregnated by Fe oxides. Abundant calcite veins oriented in several different directions are visible in some thin sections. **Middle Berriasian.**

3.2. Calcareous nannofossil biostratigraphy

A selected set of rock samples from the Nutzhof section were analysed for their calcareous nannofossil content. The succession of the nannofossil species identified in this study is represented in fig. 4. The semiquantitative study reveals that only the taxa *Nannoconus* spp., *Conusphaera* spp., *Polycostella* spp., *Cyclagelosphaera margerelii* NOËL, *Watznaueria barnesae* (BLACK) PERCH-NIELSEN, and *W. manivitae* BUKRY display significant abundances; nannofossils indicative of eutrophic environments such as *Zeugrhabdotus erectus* (DEFLANDRE) Reinhardt, *Diazomatholithus lehmannii* NOËL, and *Discorhabdus ignotus* (GÓRKA) PERCH-NIELSEN occur sporadically.

The calcareous nannofossil assemblage from the basal part of the Nutzhof section (samples 17, 18, *Tithonica* dinoflagellate Zone) contains the dissolution-resistant nannofossil species *Conusphaera mexicana* TREJO subsp. *mexicana* BRALOWER et al., (pl. 5, fig. 16), *Conusphaera mexicana* TREJO subsp. *minor* BOWN & COOPER (pl. 5, figs. 19-20), *Cyclagelosphaera margerelii* (pl. 5, fig. 11), *Cyclagelosphaera deflandrei*

(MANIVIT) ROTH (pl. 5, figs. 13), *Watznaueria barnesae* (pl. 5, fig. 7), *Watznaueria britannica* (STRADNER) REINHARDT (pl. 5, fig. 9), and *Watznaueria manivitae*. The FAD (first appearance datum) of *Faviconus multicolumnatus* BRALOWER (pl. 5, fig. 22) was recorded. The absence of the nannolith *Polycostella beckmannii* THIERSTEIN allowed us to distinguish the *Conusphaera mexicana mexicana* NJ 20 Zone; *Hexapodorhabdus cuvillieri* Subzone NJ 20-A (ROTH et al. 1983; emended BRALOWER et al. 1989) of the Early Tithonian in age.

The calcareous nannofossil assemblages from the samples 16 to 12 show dominance of the groups *Watznaueria* and *Conusphaera*. The FADs of *Zeugrhabdotus embergeri* (NOËL) PERCH-NIELSEN (pl. 5, fig. 1), *Zeugrhabdotus erectus* (pl. 5, fig. 2), and *Diazomatholithus lehmannii* were observed. The FAD of the nannolith *Polycostella beckmannii* (pl. 6, figs. 21-26) is the most significant marker indicating the base of the *Polycostella beckmannii* Subzone NJ 20-B of the *Conusphaera mexicana mexicana* Zone, NJ-20 (ROTH et al. 1983, emended BRALOWER et al. 1989). The age of this Subzone is Middle Tithonian. The range of the *Polycostella beckmannii* Subzone NJ 20-B fits with dinoflagellate *Malmica* and *Semiradiata* Zones and the lower part of the *Chitinoidella* Zone.

The calcareous nannofossils investigated in sample 11 reflect a rather distinct change. The FAD of *Helenea chiastia* WORSLEY (pl. 5, fig. 4), *Hexalithus noeliae* LOEBLICH & TAPPAN (pl. 6, fig. 30) and the nannolith species *Nannoconus compressus* BRALOWER et al. (pl. 5, figs. 23-24) are evidence for the base of the *Microstaurus chiastius* Zone NJK BRALOWER et al., 1989 and its *Hexalithus noeliae* Subzone NJK-A, which is thought to present the Late Tithonian interval. The Subzone coincides with the upper part of the *Chitinoidella* Zone.

The calcareous nannofossil assemblage selected from samples 9.0 to 6.0 contain the dissolution-resistant nannofossil genera *Conusphaera, Cyclagelosphaera, Watznaueria, Diazomatholithus* and *Assipetra*. The FAD of *Nannoconus wintereri* BRALOWER & THIERSTEIN (pl. 5, figs. 25-26) was observed (sample 9.0). Many remains of dissolution-susceptible coccoliths are present. In the upper part of the studied interval, the abundance of *Conusphaera* drops. This interval was correlated with the *Microstaurus chiastius* Zone NJK, Subzone *Rotelapillus laffitei* NJK-C, determining the J/K boundary interval. It shows good correlation with the upper part of the Late Tithonian *Crassicollaria* Zone and the *Calpionella* Zone (*Alpina* Subzone), which represent the J/K boundary interval.

The interval bearing the calpionellid species of the Lower Berriasian *Calpionella* Zone (*Ferasini* Subzone) (sample 5.0) shows a distinctive change in the calcareous nannofossil assemblage – the onset of nannoconids (*Nannoconus globulus minor* BRALOWER (pl. 5, figs. 27-28), *Nannoconus steinmanni minor* DERES & ACHÉRITÉQUY (pl. 6, fig. 1), *Nannoconus kamptneri minor* BRALOWER, *Nannoconus cornuta* DERES & ACHÉRITÉQUY (pl. 5, figs. 29). This nannofossil event indicates the base of the *Nannoconus steinmannii minor* Subzone NJK-D (*Microstaurus chiastius* Zone NJK) BRALOWER et al., which is lowermost Berriasian in age.

The calcareous nannofossils studied from the sample interval 4.2 – 0.0 (correlating with the calpionellid *Calpionella* Zone, *Elliptica* Subzone) reveal the diversification of nannoconids. The FAD of *Nannoconus steinmanni steinmanni* KAMPTNER (pl. 5, fig. 30; pl. 6, figs. 4, 8,9) was registered. It could reflect the explosion in nannoconid abundance

(sensu BRALOWER et al. 1989: p. 188). *Nannoconus globulus minor* (pl. 6, figs. 7, 11), *Nannoconus kamptneri minor* (pl. VI. figs. 2, 3), *Nannoconus wintereri*, *Nannoconus globulus* BRÖNNIMANN subsp. *globulus* DERES & ACHÉRITÉQUY (pl. 6, fig. 5), *Nannoconus steinmanni minor* DERES & ACHÉRITÉQUY (pl. 6, figs. 1, 13, 16-18), *Nannoconus steinmanni steinmanni* (pl. 6, figs. 19-20), and *Nannoconus kamptneri kamptneri* BRÖNNIMANN (pl. 6, figs. 2-3, 6, 15), *Nannoconus* spp. (pl. 6, figs. 12), indicated the *Nannoconus steinmannii steinmannii* Zone NK-1, BRALOWER et al., 1989, which is Middle Berriasian in age.

Based on the calcareous nannofossil distribution, the interval between the FO of *Nannoconus wintereri* co-occurring with small nannoconids (sample 9.0) and the FO of *Nannoconus steinmanni minor* in sample 5.0 (FAD after HARDENBOL et al. 1998 – 143.92 Ma) can be interpreted in the Nutzhof section as the Tithonian-Berriasian boundary interval.

3.3. Cephalopod fauna

The cephalopod fauna from the Blassenstein Formation, correlated with micro- and nannofossil data from the marl-limestone succession, indicates Early Tithonian to Middle Berriasian age (*Hybonoticeras hybonotum* Zone up to the *Subthurmannia occitanica* Zone). According to the correlation of the fossil and magnetostratigraphic data, the entire log of the Nutzhof section embraces a duration of approx. 7 million years (approx. 150 – 143 mya). Six different genera were recorded, each apparently represented by a single species. The occurrence at the Nutzhof section is dominated by ammonites of the perisphinctid-type. Ammonitina are the most frequent component (60 %; *Subplanites* and *Haploceras*), followed by the Phylloceratina (25 %; *Ptychophylloceras* and *Phylloceras*), and the Lytoceratina (15; represented by *Lytoceras* and *Leptotetragonites*). The cephalopod fauna consists solely of Mediterranean elements (for more details see LUKENEDER 2009; this volume).

4. Discussion

The high-resolution quantitative analysis of selected organic groups (radiolarians, saccocomids, calpionellids) indicates major variations in their abundance and composition (fig. 2). While the Upper Jurassic settings of the Nutzhof section were more or less influenced by the periodic input of biodetritus from surrounding shallow marine palaeoenvironments, the Berriasian settings were more equalized: the pelagic sediments were predominantly composed of remnants of planktonic microorganisms (radiolarians, calpionellids, dinoflagellates and nannofossils).

The calcareous dinoflagellates predominate in the Lower and Upper Tithonian sequence (Fig. 3), being represented by *Cadosina parvula* NAGY, *Carpistomiosphaera borzai* (NAGY), *Schizosphaerella minutissima* (COLOM), *Parastomiosphaera malmica* (BORZA), *Cadosina semiradiata semiradiata* WANNER, *Cadosina semiradiata fusca* (WANNER), *Carpistomiosphaera tithonica* NOWAK, *Colomisphaera fortis* ŘEHÁNEK, *Colomisphaera tenuis* (NAGY), *Colomisphaera carpathica* (BORZA), and *Stomiosphaerina proxima* ŘEHÁNEK. Several dinoflagellate zones were recognizable: *Tithonica*, *Malmica* and *Semiradiata* Zones. For the first time the appearance of *Colomisphaera fortis* ŘEHÁNEK

precedes the appearance of *Colomisphaera tenuis* (NAGY), preventing the determination of the *Tenuis* and *Fortis* dinoflagellate Zones sensu ŘEHÁNEK (1992).

The stratigraphic and palaeoecological potential of calcareous dinoflagellates has been discussed by REHÁKOVÁ (2000a, b). In the Nutzhof section, the Lower Tithonian record of these microorganisms shows a distinct change in abundance and composition. Orthopithonellid forms dominated in the *Tithonica* and *Malmica* Zones, but were replaced by obliquipithonellid species dominated by *Cadosina semiradiata semiradiata* WANNER in the *Semiradiata* Zone. According to MICHALÍK et al. (in print), coinciding acme peaks of *Cadosina semiradiata semiradiata* WANNER and *Conusphaera* spp. probably indicate warmer surface waters.

Based on the vertical calpionellid distribution, the J/K boundary interval can be characterized by several calpionellid events – the onset, diversification, and extinction of chitinoidellids (Middle Tithonian); the onset, burst of diversification, and extinction of crassicollarians (Late Tithonian); and the onset of the monospecific *Calpionella alpina* association just at the J/K boundary (REHÁKOVÁ in MICHALÍK et al., in print).

Chitinoidellids in the Nutzhof section (fig. 3) are very rare, being represented by *Borziella slovenica* (BORZA), *Dobeniella tithonica* (BORZA) and *Chitinoidella boneti* DOBEN, species typical for the *Boneti* Subzone of the *Chitinoidella* Zone. The appearance of first hyaline calpionellid loricas represented by *Praetintinnopsella andrusovi* BORZA and *Tintinnopsella remanei* BORZA precede the crassicolarian radiation. *Crassicollaria parvula* REMANE and *Calpionella alpina* LORENZ dominate over *Crassicollaria massutiniana* (COLOM), *Calpionella grandalpina* NAGY and *Tintinnopsella carpathica* (MURGEANU & FILIPESCU) in the *Remanei* Subzone of the *Crassicollaria* Zone. The interval with the monospecific calpionellid association consisting predominantly of *Calpionella alpina* LORENZ was also identified in the section. A similar interpretation of calpionellid evolution and the biostratigraphy of the Jurassic-Cretaceous boundary interval was given by REMANE (1986), POP (1994), REHÁKOVÁ (1995), OLÓRIZ et al. (1995), GRÜN & BLAU (1997), and ANDREINI et al. (2007).

Despite the inconvenient lithology, the calcareous nannofossil distribution in the Nutzhof section showed its potential for a stratigraphy of the deposits of the J/K boundary interval.

The major role of the coccoliths of the family Watznaueriaceae and three nannolithic genera (*Conusphaera*, *Nannoconus*, and *Polycostella*) was evident in the assemblage composition, which is in agreement with the results of nannofossil studies in other locations at low latitudes across the J/K boundary (THIERSTEIN 1971, 1973, 1975; ERBA 1989; GARDIN & MANIVIT 1993; ÖZKAN 1993; TAVERA et al. 1994; BORNEMANN et al. 2003; PSZCZÓŁKOWSKI & MYCZYŃSKI 2004; TREMOLADA et al. 2006; HALÁSOVÁ in MICHALÍK et al. in print.).

The first occurrences of nannofossils are perhaps somewhat unreliable due to the bad conditions of preservation, but we tentatively determined the boundaries of zones and subzones based on certain stratigraphic markers (*Polycostella beckmannii*, *Helenea chiastia*, *Hexalithus noeliae*, *Nannoconus wintereri*, *Nannoconus globulus minor*, *Nannoconus steinmanni minor*, *Nannoconus kamptneri minor*, *Nannoconus steinmanni steinmanni*, *Nannoconus kamptneri kamptneri*, *Nannoconus globulus globulus*).

TREMOLADA et al. (2006) detected that *Conusphaera* dominates the nannolith assemblage in the late Middle Tithonian ("*Conusphaera* world"). This agrees with data obtained in the Nutzhof section. The acme peak of the genus *Polycostella* in samples 13.0 and 14.0 coincides with the Middle Tithonian *Semiradiata* Subzone (REHÁKOVÁ 2000b). If compared with the Brodno section (MICHALÍK et al. 2007 and MICHALÍK et al. in print), the dominance of the Brodno nannoliths represented by *Polycostella beckmannii* was somewhat higher in the *Chitinoidella* Zone. The first appearance of *Helenea chiastia* also shows a similar diachroneity: it was identified in the Brodno section close to the onset of the calpionellid *Crassicolaria* Zone, whereas in the Nutzhof section its first appearance was recorded in the uppermost part of the *Chitinoidella* Zone.

The most distinct nannofossil event was observed in the lowermost Berriasian (in the interval of calpionellid *Calpionella* Zone, *Ferasini* Subzone of the Lower Berriasian age), the onset of nannoconids. This indicates the change in the palaeooceanographic regime and, from the biostratigraphic point of view, the upper J/K boundary datum based on the nannofossils (BORNEMANN et al., 2003).

Most of the ammonite specimens were apparently not redeposited from shallower shelf regions into a deeper shelf environment. The ammonite fauna of the Nutzhof section is interpreted as an assemblage comprising only "autochthonous" and parautochthonous pelagic elements from the open sea. The ammonite shells found their final resting place on the deeper shelf or upper slope of the European side of the Penninic Ocean.

5. Conclusions

The biostratigraphic study based on the distribution of calpionellids allowed us to distinguish the *Boneti* Subzone of the *Chitinoidella* Zone in the Nutzhof section. The J/K boundary in this section is situated between the *Crassicollaria* and *Calpionella* Zone (interval limited by samples 7.0 – 5.6). This base is defined by the morphological change of *Calpionella alpina* tests. The base of the *Crassicollaria* Zone approximately coincides with the onset of *Tintinnopsella remanei* BORZA and the base of the standard *Calpionella* Zone, with the monospecific calpionellid association being dominated by *Calpionella alpina* LORENZ. Two further Subzones (*Ferasini* and *Elliptica*) of the standard *Calpionella* Zone were recognized in radiolarian-calpionellid and calpionellid-radiolarian wackestones in the overlying topmost part of the investigated sequence.

Calcareous nannofossils from the Nutzhof section belong to low poorly diversified, because of the lithology. Nonetheless, the appearance of several important genera was determined, allowing the studied deposits to be attributed to the Early, Middle and Late Tithonian, the approximation of the Tithonian-Berriasian boundary, and the definition of the Early Berriasian nannofossil zones. The results show the major role of the coccoliths of the family Watznaueriaceae and nannoliths of the genera *Conusphaera*, *Nannoconus* and *Polycostella* in the assemblage composition. The interval between the FAD of *Nannoconus wintereri* co-occurring with small nannoconids in sample No 9 (the uppermost Tithonian) and the FAD of *Nannoconus kamptneri minor* in sample No 5 (lowermost Berriasian; 143.92 Ma after HARDENBOL et al. 1998) is interpreted as the Tithonian-Berriasian boundary interval. The nannoconid dominance ("*Nannoconus*

world", TREMOLADA et al. 2006) starts, also in Nutzhof profile, in the lowermost Berriasian.

The macrofauna is represented especially by ammonoids, belemnoids, aptychi and bivalves. The whole section yielded about 46 ammonites. The sparse and selective occurrence of the ammonites within the Nutzhof log and the lithologic character of the Formation made sampling difficult.

The stratigraphic investigation of the cephalopods, microfauna and nannofauna revealed that the Nutzhof section comprises Tithonian to Berriassian sediments. The ammonoid fauna solely contains descendants of the Mediterranean Province. The ammonite fauna comprises 6 different genera, dominated by the perisphinctid-type. Ammonitina are the most frequent component (60 %; *Subplanites* and *Haploceras*), followed by the Phylloceratina (25 %; *Ptychophylloceras* and *Phylloceras*), and the Lytoceratina (15 %; represented by *Lytoceras* and *Leptotetragonites*). The cephalopod fauna consists solely of Mediterranean elements. The described descendants of *Subplanites* display the first evidence of these ammonoids within the Gresten Klippenbelt.

The cephalopod fauna from the Nutzhof section correlated with micro- and nannofossil data from the marl-limestone succession, indicating Early Tithonian to Middle Berriasian age (*Hybonoticeras hybonotum* Zone up to the *Subthurmannia occitanica* Zone). According to the correlation of the fossil and magnetostratigraphic data, the entire log of the Nutzhof section embraces a duration of approx. 7 million years (approx. 150 – 143 mya).

Acknowledgments

The authors thank to SEVINÇ ÖZKAN-ALTINER (Ankara), GLORIA ANDREINI (Perugia) and ANDREAS KROH (Vienna) for their valuable remarks and comments. Sincere thanks go to HANS EGGER (Vienna) for showing us the outcrop. This research was supported by the Grant Agency for Sciences in Slovakia APVV (projects APVV-0280-07, APVV-0248-07, APVV-0465-06 and APVV-51-011305). We also gratefully acknowledge the Austrian Science Fund (FWF) for the financial support of project P20018-N10. Photographic work was done by ALICE SCHUMACHER (Natural History Museum, Vienna).

References

ANDREINI, G., CARACUEL J. E. & PARISI, G. (2007): Calpionellid biostratigraphy of the Upper Tithonian – Upper Valanginian interval in Western Sicily (Italy). – Swiss Journal of Geosciences, **100**: 179-198.

BORNEMANN, A., ASCHWER, U. & MUTTERLOSE, J. (2003): The impact of calcareous nannofossils on the pelagic carbonate accumulation across the Jurassic–Cretaceous boundary interval. – Palaeogeography, Palaeoclimatology, Palaeoecology, **199**: 187-228.

BRALOWER, T. J., MONECHI, S. & THIERSTEIN, H. R. (1989): Calcareous nannofossil zonation of the Jurassic-Cretaceous boundary interval and correlation with the geomagnetic polarity timescale. – Marine Micropaleontology, **14**: 153-235.

CŽJŽEK, J. (1852): Aptychenschiefer in Niederösterreich. – Jahrbuch der Kaiserlich-Königlich Geologischen Reichs-Anstalt, **3**: 1-7.

ERBA, E. (1989): Calcareous nannofossil zonation of the Jurassic-Cretaceous boundary interval and correlation with the geomagnetic polarity timescale. – Marine Micropaleontology, **14**: 153-235.

GARDIN, S. & MANIVIT, H. (1993): Upper Tithonian and Berriasian calcareous nannofossils from the Vocontian Trough (SE France): Biostratigraphy and sequence stratigraphy. – Bulletin des Centres de Recherches Exploration – Production Elf-Aquitaine, **17**/1: 277-289.

GRÜN, B., & BLAU, J. (1997): New aspects of calpionellid biochronology: proposal for a revised calpionellid zonal and subzonal division. – Revue de Paléobiologie, **16**: 197-214.

HARDENBOL, J., THIERRY, J., FARLEY, M. B., JACQUIN, T., DE GRACIANSKY, P. C. & VAIL, P. R. (1998): Mesozoic and Cenozoic sequence stratigraphy of European basins. – SEMP, Special Publications, **60**, 1998. Tulsa.

KÜPPER, H. (1962): Beobachtungen in der Hauptklippenzone bei Stollberg, N.Ö. – Verhandlungen der Geologischen Bundesanstalt, **2**: 263-268.

MICHALÍK , J., REHÁKOVÁ, D., HALÁSOVÁ, E. & LINTNEROVÁ, O. (2007): Integrated stratigraphy of the Jurassic/Cretaceous boundary at the Brodno section (the Kysuca Unit, Pieniny Klippen Belt, Western Carpathians). – Abstract book, International geological correlation programme 506 – Jurassic marine: non-marine correlation, University of Bristol, p. 3.

––– , REHÁKOVÁ, D., HALÁSOVÁ, E. & LINTNEROVÁ, O. (in print): A possible West Carpathian regional stratotype of the Jurassic/Cretaceous boundary (the Brodno section near Žilina). – Geologica Carpathica.

OLÓRIZ, F., CARACUEL, J. E., MARQUES, B. & RODRÍGUEZ-TOVAR, F. J. (1995): Asociaciones de Tintinnoides en facies Ammonitico Rosso de la Sierra Norte (Mallorca). – Revista Españolade Paleontología, No. Homenaje al Dr. G. COLOM, 77-93.

ÖZKAN, S. (1993): Calcareous nannofossils from the Late Jurassic-Early Cretaceous of Northwest Anatolia, Turkey. – Geological Journal, **28**/3-4: 295-307.

POP, G. (1994): Calpionellid evolutive events and their use in biostratigraphy. – Romanian Journal of Stratigraphy **76**: 7-24.

––– (1997) : Révision systématique des chitinoidelles tithoniennes des carpathes méridionales (Roumanie). – Compte Rendus de l´Académie des Sciences, Paris, Série II a, **342**: 931-938.

PSZCZÓŁKOWSKI, A. & MYCZYŃSKI, R. (2004): Ammonite-supported microfossil and nannoconid stratigraphy of the Tithonian-Hauterivian limestones in selected sections of the Branisko Succession, Pieniny Klippen Belt (Poland). – Studia Geologica Polonica, **123**: 133-197.

PRUNER, P., SCHNABL, P., & LUKENEDER, A. (2009): Preliminary results of magnetostratigraphic investigations across the Jurassic/Cretaceous boundary strata in the Nutzhof, Austria. – Berichte der Geologischen Bundesanstalt, **74**: 83-84.

REHÁKOVÁ, D. (1995): New data on calpionellid distribution in the Upper Jurassic/Lower Cretaceous formations (Western Carpathians). – Mineralia Slovaca, **27**: 308-318. [In Slovak].

––– & MICHALÍK, J. (1997): Evolution and distribution of calpionellids – the most characteristic constituents of Lower Cretaceous tethyan microplankton. – Cretaceous Research **18**: 493-504.

––– (1998): Calpionellid genus *Remaniella* CATALANO 1956 in Lower Cretaceous pelagic deposits of Western Carpathians. – Mineralia Slovaca, **30**: 443-452.

––– (2000a): Evolution and distribution of the Late Jurassic and Early Cretaceous calcareous dinoflagellates recorded in the Western Carpathian pelagic carbonate facies. – Mineralia Slovaca, **32**: 79-88.

——— (2000b): Calcareous dinoflagellate and calpinellid bioevents versus sea-level fluctuations recorded in the West-Carpathian (Late Jurassic/ Early Cretaceous) pelagic environments. – Geologica Carpathica, **51**/4: 229-243.

——— (2002): Chitinoidella TREJO, 1975 in Middle Tithonian carbonate pelagic sequences of the West Carpathian tethyan area. – Geologica Carpathica, **55**/6: 369-379.

——— , HALÁSOVÁ, E. & LUKENEDER, A. (2009): The Jurassic-Cretaceous boundary in the Austrian Klippen Belt (Nutzhof, Lower Austria): Implications on micro- and nannofacies analysis. – Berichte der Geologischen Bundesanstalt, **74**: 95-95.

ŘEHÁNEK, J. (1992): Valuable species of cadosinids and stomiosphaerids for determination of the Jurassic-Cretaceous boundary (vertical distribution, biozonation). – Scripta, **22**: 117-122.

REMANE, J. (1986): Calpionellids and the Jurassic-Cretaceous boundary. – Acta Geologica Hungarica, **29**: 15-26.

ROTH, P. H., MEDD, A. W. & WATKINS D,. K. (1983): Jurassic calcareous nannofossil zonation, an overview with new evidence from Deep Sea Drilling Project Site 534A. In Sheridan R.E., Gradstein F.M. et al., Initial Reports DSDP **76**: 573-579.

TAVERA J. M., AGUADO R., COMPANY M. & OLÓRIZ F. (1994): Integrated biostratigraphy of the. Durangites and Jacobi Zones (J/K boundary) at the Puerto Escaño section in Southern Spain (province of Cordoba). – Geobios, M.S., **17**: 469-476.

THIERSTEIN, H. (1971). Tentantive Lower Cretaceous Calcareous Nanoplankton Zonation. – Eclogae Geologicae Helvetiae, **64**, 3: 437-652.

——— (1973). Lower Cretaceous Calcareous Nannoplankton Biostratigraphy. – Abhandlungen der Geologischen Bundesanstalt, **29**: 3-52.

——— (1975): Calcareous nannoplankton biostratigraphy at the Jurassic-Cretaceous boundary. Colloque sur la Limite Jurassique-Crétacé. – Bureau de Recherches Géologique et Minières, Mémoires, **86**: 84-94.

TREMOLADA F., BORNEMANN A., BRALOWER T., KOEBERL C., VAN DE SCHOOTBRUGGE B. (2006): Paleoceanographic changes across the Jurassic/Cretaceous Boundary: the calcareous phytoplankton response. Earth and Planetary Science Letters **241**: 361-371.

Appendix

Nutzhof section – microfacies analysis of thin sections studied

No. 18.0
Bioturbated mudstone – rare radiolarians, sponge spicules, aptychy and ostracod fragments. Matrix penetrated by thin calcite veins.

No. 17.8
Bioturbated mudstone – rare *Saccocoma* sp., calcified radiolarians and sponge spicules, aptychy and ostracod fragments. Biodetritus are concentrated in nests and irregular fine grained layers which are rich in Fe-hydroxides.

No. 17.6
Bioturbated mudstone – rare *Saccocoma* sp., calcified radiolarians. Biodetritus is concentrated in nests which are rich in Fe- oxydes/hydroxides. Matrix is stylolitized; there are many composed stylolites and also thin calcite veins penetrating biomicrite mudstone.

No. 17.4
Bioturbated mudstone. Biodetrit increases in abundance. There are sponge spicules, rare *Saccocoma* sp., aptychy, crinoid fragments, *Cadosina parvula* and *Schizosphaerella minutissima* observed in thin section. Silty glauconit is also visible.

No. 17.4
Bioturbated mudstone – *Saccocoma* sp., aptychy, crinoids, sponge spicules, (without radiolarians), also *Cadosina parvula* and *Schizosphaerella minutissima*, glauconite of silt size.

No. 17.2
Bioturbated mudstone. *Carpistomiosphaera borzai*, *Schizosphaerella minutissima*, *Saccocoma* sp., aptychy, crinoids, sponge spicules, radiolarians (many of them are pyritized), ostracods. Matrix is stylolitized. ***Tithonica* Zone**

No 17.0
Bioturbated mudstone with rare organic fragments – *Saccocoma* sp., *Cadosina semiradiata semiradiata*, *Parastomiosphaera malmica*, *Schizosphaerella minutissima*, ostracods. Matrix penetrated by thin calcite veins. ***Malmica* Zone**.

No. 16.8
Mudstone with rare biofragments. It contains *Saccocoma* sp., *Cadosina semiradiata semiradiata*, *Parastomiosphaera malmica*, *Schizosphaerella minutissima*, *Dentalina* sp., bivalves, ostracods, framboidal pyrit and glauconit. Thin laminae composed of fine frained silt with muscovite and clay minerals are documented in the thin section.

No. 16.6
Bioturbated mudstone with rare skeletal fragments – ostracods, calcified radiolarians, *Saccocoma* sp., *Cadosina semiradiata semiradiata*, *Parastomiosphaera malmica*, *Schizosphaerella minutissima*, *Carpistomiosphaera tithonica*, Matrix is rich in stylolites.

No. 16.4
Marly limestone – mudstone with fine grained biofragments dispersed in matrix. It contains *Parastomiosphaera malmica*, *Cadosina semiradiata fusca*, *Cadosina semiradiata semiradiata*, *Saccocoma* sp., ostracods, silty glauconit and abundant pyrit.

No. 16.2
Bioturbated mudstone with *Saccocoma* sp., *Parastomiosphaera malmica*, *Cadosina semiradiata fusca* and ostracods. Pyrit is concentrated into the nests, there are several layers rich in silted admixure with glauconite and muscovite.

No. 16,0
Mudstone. Marly matrix with peletic structure (content of bio fragments is very low). It contains *Parastomiosphaera malmica* (one cyst in thin section) and glauconite.

No. 15.8
Bioturbated mudstone with nests rich in pyrite accumulations. It contains sponge spicules, radiolarians, bivalves, *Cadosina semiradiata semiradiata*, *Parastomiosphaera malmica*, *Spirilina* sp., *Saccocoma* sp.

No. 15.6
Marly biomicrite limestone with laminae of parallel oriented biodetrite – *Saccocoma* sp., *Parastomiosphaera malmica*, *Schizosphaerella minutissima*, *Cadosina semiradiata semiradiata*, ophiurid fragment, ryncholite, bivalves and ostracods.

No. 15.6
Marly biomicrite limestone with laminas of oriented biodetrite – *Saccocoma* sp., *Parastomiosphaera malmica*, *Schizosphaerella minutissima*, *Cadosina semiradiata semiradiata*, ophiuroid fragment, rhyncholit, sponge spicules, bivalves and ostracods, glauconite and pyrite.

No. 15.4
Bioturbated marly biomicrite limestone with laminas of oriented biodetrite – *Saccocoma* sp., *Parastomiosphaera malmica*, *Schizosphaerella minutissima*, *Dentalina* sp., ostracods and foraminifers. Matrix is stylolitized.

No. 15.2
Bioturbated mudstone – radiolarians, ostracods, foraminifers, *Saccocoma* sp., *Parastomiosphaera malmica*. Matrix is penetrated by thin calcite veins and stylolites impregnated by Fe-minerals.

No. 15.0
Bioturbated biomicrite limestone to mudstone. It contains *Parastomiosphaera malmica*. Pyrite is accumulated in nests.

No. 14.8
Bioturbated mudstone with distinct gradation. Radiolarians increase in abundance. It contains also aptychy fragments.

No. 14.6
Biomicrite limestone – mudstone with *Saccocoma* sp., ostracods, crinoids, *Parastomiosphaera malmica*, *Cadosina semiradiata semiradiata*, *Schizosphaerella minutissima*, juvenile ammonite.
***Semiradiata* Zone**

No. 14.4
Bioturbated mudstone with the nests riched in radiolarians, aptychy, ostracods, *Saccocoma* sp., *Parastomiosphaera malmica*, *Cadosina semiradiata semiradiata* and *Schizosphaerella minutissima*.

No. 14.2
Bioturbated mudstone with ostracods, *Saccocoma* sp., radiolarians, sponge spicules, frequent *Parastomiosphaera malmica*. Biofragments are impregnated by pyrit. Matrix contains also silty glauconit.

No. 14.0
Bioturbated mudstone penetrated by abundant calcite veins. It contains calcified radiolarians, ostracods, *Saccocoma* sp. Fe-minerals impregnate biodetrite fragments and stylolites.

No. 13.7
Bioturbated mudstone with tiny layers rich in silty admixure. It contains ostracods, radiolarians, crinoids, bivalves, *Saccocoma* sp., *Parastomiosphaera malmica*, *Cadosina semiradiata semiradiata*, *Schizosphaerella minutissima*, framboidal pyrite and glauconit.

No. 13.6
Mudstone – aptychy, bivalve, radiolarians impregnated by Fe-oxydes, abundant *Parastomiosphaera malmica*, *Carpistomiosphaera borzai*, *Schizosphaerella minutissima*.

No. 13.4
Marly limestone – mudstone – *Parastomiosphaera malmica*, *Cadosina semiradiata semiradiata*, pyrite and glauconite. Matrix brings the marks of synsedimentary deformation.

No. 13.2
Mudstone with thin layers rich in biodetrite. It contains foraminifers, ostracods, *Parastomiosphaera malmica* and *Cadosina semiradiata semiradiata*.

No. 13.0
Bioturbated mudstone with *Saccocoma* sp., foraminifers, *Parastomiosphaera malmica, Cadosina semiradiata semiradiata*, aptychy, crinoids and nests of pyrite. Matrix is fine grained, composed mainly of nannofossils. It is localy micropeletic.

No. 12.8
Mudstone – small fragments of biodetrite are localy concentated into fine laminae. Limestone contains *Saccocoma* sp., *Schizosphaerella minutissima*, *Parastomiosphaera malmica*, foraminifers, crinoids, aptychy, ostracods, glauconite and pyrite.

No. 12.6
Mudstone with *Parastomiosphaera malmica*, *Saccocoma* sp., aptychy, crinoids, radiolarians, bivalves. Matrix is stylolitised and it contains nests of pyrite and calcite veins of several generation (also raster types of calcite veins are present). Fe oxydes/hydroxides impregnate biofragments.

No. 12.4
Mudstone – *Parastomiosphaera malmica*, radiolarians, sponge spicules, ostracods, foraminifers, bivalves. Silty glauconite, nests of pyrite, stylolites, calcite veins.

No. 12.2
Mudstone – there are marks of synsedimentary deformation visible in the lower part of the thin section. *Parastomiosphaera malmica*, *Schizosphaerella minutissima*, *Cadosina semiradiata semiradiata* and silty glauconite are present.

No. 12.0
Mudstone – radiolarians, sponge spicules, *Cadosina semiradiata semiradiata*. nests of pyrite, stylolites, calcite veins.

No. 11.8
Mudstone – with frequent biodetrite concentrated in its lower part. Radiolarians, sponge spicules, abundant *Cadosina semiradiata semiradiata*, *Colomisphaera pulla*, *Parastomiosphaera malmica*. Matrix build predominantly by nannofossils.

No. 11.6
Biomicrite limestone – mudstone with input of skeletal debris concentrated in thin laminae. *Saccocoma* sp., *Colomisphaera fortis*, *Parastomiosphaera malmica*, *Schizosphaerella minutissima*, *Cadosina semiradiata semiradiata*, *Cadosina semiradiata fusca*, *Borziella slovenica*, *Dobeniella tithonica*, *Chitinoidella boneti*, aptychy, bivalves, ostracods, glauconite, pyrite. Part of thin section rich in biodetritus is limited by the thin clay laminae and slowly pass to micrite limestone which is penetrated by abundant calcite veins. ***Chitinoidella* Zone**.

No. 11.4
Micrite mudstone – *Saccocoma* sp., *Cadosina semiradiata semiradiata*, ostracods, crinoids, glauconite. Locally accumulations of pyrite cubes.

No. 11.2
Mudstone – with thin laminae rich in biodetrite – small fragments of crinoids, ostracods, aptychy, *Cadosina semiradiata semiradiata*, *Schizosphaerella minutissima*, *Colomisphaera fortis*. Fine clay admixture, pyrite, glauconite.

No. 11.0
Mudstone – small fragments of ostracods (partly with ornamented shells), crinoids, foraminifers, ophiurids, sponge spicules, aptychy, *Saccocoma* sp., *Cadosina semiradiata semiradiata*, *Borziella slovenica*, stylolites, glauconite, pyrite.

No. 10.8
Bioturbated mudstone penetrated by thin calcite veins. Radiolarians, ostracods, crinoids, sponge spicules, bivalves, foraminifers, *Cadosina semiradiata semiradiata*, *Schizosphaerella minutissima*, *Colomisphaera fortis*, *Colomisphaera tenuis*, *Praetintinnopsella andrusovi*, glauconite, pyrite. ***Praetintinnopsella* Zone**.

No. 10.6
Bioturbated mudstone with laminae of fine detrite. *Saccocoma* sp., *Cadosina semiradiata semiradiata*, radiolarians, crinoids, glauconite, pyrite, sponge spicules, bivalves. Nests of framboidal pyrite.

No. 10.4
Bioturbated mudstone passing to radiolarian–sponge wackestone with radiolarians, sponge spicules, ostracods, *Cadosina semiradiata semiradiata*, *Colomisphaera carpathica*.

No. 10.2
Bioturbated mudstone with laminae of fine biodetrite rich in calcareous cysts – *Cadosina semiradiata semiradiata*. It contains also *Tintinnopsella remanei* – the index species of ***Remanei* Subzone** of ***Crassicollaria* Zone**.

No. 10.1
Mudstone with laminae of fine detrite accumulation. It contains radiolarians, sponge spicules, ostracods, *Tintinnopsella remanei*, *Cadosina semiradiata semiradiata*, *Cadosina semiradiata fusca*, *Schizosphaerella minutissima*, *Parastomiosphaera malmica*. Matrix penetrated by abundant thin calcite veins.

No. 10.0
Radiolarian-calpionella wackestone passing to radiolarian packstone (in small chert accumulation). *Calpionella alpina* (loricas are coated by microgranular calcite dark in colour).

No. 9.8
Radiolarian-calpionella wackestone – *Calpionella alpina*, *Calpionella grandalpina*, *Crassicollaria parvula*, *Crassicollaria massutiniana*, *Tintinnopsella carpathica*, *Colomisphaera carpathica*, aptychy, foraminifers, radiolarians and bivalves.

No. 9.6
Radiolarian-calpionella wackestone with *Calpionella grandalpina*, *Calpionella alpina*, *Crassicollaria parvula*, *Tintinnopsella carpathica*, *Schizosphaerella minutissima*, aptychy, bivalves, sponge spicules. Nests of pyrite and calcite veins of different orientation.

No. 9.4
Radiolarian-calpionella wackestone. *Calpionella alpina, Crassicollaria massutiniana, Crassicollaria parvula, Stomiosphaerina proxima*, radiolarians, crinoids, bivalves, aptychy. Matrix is penetrated by rich calcite veins of different orientation, filled by blocky and fibrous calcite crystals.

No. 9.2
Calpionella-radiolarian wackestone – *Crassicollaria parvula, Calpionella alpina, Cadosina semiradiata fusca, Colomisphaera fortis*, aptychy, bivalves, sponge spicules, radiolarians, pyrite, foraminifers and abundant calcite veins.

No. 9.0
Radiolarian-calpionella wackestone. Radiolarians, sponge spicules, crinoids, *Calpionella alpina, Crassicollria parvula*.

No. 8.8
Radiolarian-calpionella wackestone. Crinoids, sponge spicules, bivalves, aptychy, *Calpionella alpina, Crassicollaria parvula*.

No. 8.6
Radiolarian-calpionella wackestone. Crinoids, sponge spicules, bivalves, *Crassicollaria parvula, Calpionella alpina, Stomiosphaerina proxima*.

No. 8.4
Radiolarian-calpionella wackestone. Sponges, crinoids, *Colomisphaera fortis, Schizosphaerella minutissima, Calpionella alpina, Crassicollaria parvula, Tintinnopsella carpathica*.

No. 8.2
Radiolarian-calpionella wackestone. Frequent *Cadosina semiradiata fusca*, radiolarians, sponges, bivalves, *Calpionella alpina, Tintinnopsella carpathic* and *Crassicollaria parvula*.

No. 8.0
Radiolarian-calpionella wackestone. Radiolarians decrease in abundance. *Calpionella alpina, Crassicollaria parvula*, aptychy, bivalves, crinoids, ostracods. Matrix penetrated by thin calcite veins.

No. 7.8
Radiolarian-calpionella wackestone. Radiolarians, foraminifers, bivalves, ostracods, aptychy, *Calpionella alpina, Tintinnopsella carpathica, Cadosina semiradiata fusca* and veins filled by calcite.

No. 7.6
Radiolarian-calpionella wackestone. Radiolarians, aptychy, bivalves, ostracods, *Calpionella alpina, Tintinnopsella carpathica* and *Crassicollaria parvula*.

No. 7.4
Radiolarian-calpionella wackestone. Radiolarians, sponges, crinoids, aptychy, bivalves, ostracods, foraminifers, *Calpionella alpina, Tintinnopsella carpathica, Crassicollaria parvula, Cadosina semiradiata fusca* and calcite veins.

No. 7.2
Radiolarian-calpionella wackestone. Radiolarians, bivalves, crinoids, foraminifers, *Calpionella alpina, Tintinnopsella carpathica, Crassicollaria parvula, Stomiosphaerina proxima, Schizosphaerella minutissima, Cadosina semiradiata fusca* and calcite veins.

No. 7.0
Calpionella-radiolarian wackestone – radiolarians dominated over *Calpionella alpina* (monospecific association of *Calpionella alpina*), aptychy, bivalves, sponges – **J/K boundary** – ***Alpina*** **Subzone** of ***Calpionella*** **Zone**.

No. 6.8
Calpionella mudstone – *Calpionella alpina,* aptychy, in lower part of the thin section radiolarians are also present.

No. 6.6
Mudstone penetrated by calcite veins. Biodetrite is not frequent. Radiolarians, *Calpionella alpina*, aptychy, bivalves and crinoids.

No. 6.4
Mudstone penetrated by rich thin calcite veins of different orientation. Radiolarians, *Calpionella alpina*, ostracods, bivalves and crinoids.

No. 6.2
Radiolarian-calpionella wackestone. *Calpionella alpina*, *Tintinnopsella carpathica*, radiolarians, *Schizosphaerella minutissima*, bivalves and crinoids.

No. 6.0
Calpionella-radiolarian wackestone. Crinoids, radiolarians, aptychy, bivalves, *Calpionella alpina* (typical Early Berriasian forms), *Tintinnopsella carpathica* and *Stomiosphaerina proxima*.

No. 5.8
Radiolarian-calpionella wackestone. Radiolarians, aptychy, bivalves, crinoids, ostracods, foraminifers, *Calpionella alpina, Tintinnopsella carpathica*. Calcite veins.

No. 5,6
Radiolarian-calpionella wackestone. Crinoids, aptychy (in average 1 or 2 pieces in thin section) radiolarians, *Calpionella alpina*, *Tintinnopsella carpathica* and *Lorenziella hungarica*.

No. 5.4
Radiolarian-calpionella wackestone. Radiolarians, crinoids, aptychy, *Calpionella alpina*, *Tintinnopsella carpathica*, *Remaniella ferasini*, *Remaniella duranddelgai*. Matrix is penetrated by calcite veins. ***Ferasini*** **Subzone** of the ***Calpionella*** **Zone**.

No. 5.2
Calpionella wackestone. Less radiolarians, aptychy, bivalves, crinoids, *Calpionella alpina*, *Tintinnopsella carpathica*, *Lorenziella hungarica*, *Cadosina semiradiata fusca* and *Schizosphaerella minutissima*.

No. 5.0
Radiolarian-calpionella wackestone. Radiolarians, aptychy, bivalves, *Calpionella alpina*, *Tintinnopsella carpathica* and *Remaniella ferasini*.

No. 4.8
Radiolarian-calpionella wackestone. Radiolarians, *Calpionella alpina*, *Tintinnopsella carpathica*, *Schizosphaerella minutissima* and bivalves.

No. 4.6
Radiolarian-calpionella wackestone. Radiolarians, bivalves, aptychy, crinoids, *Calpionella alpina*, *Tintinnopsella carpathica* and *Schizosphaerella minutissima*.

No. 4.4
Calpionella-radiolarian wackestone. Radiolarians, aptychy, bivalves, ostracods, *Remaniella catalanoi*, *Remaniella duranddelgai*, *Calpionella alpina* and *Tintinnopsella carpathica*.

No. 4.2
Radiolarian-calpionella wackestone. *Calpionella alpina*, *Calpionella elliptica*, *Tintinnopsella carpathica*, *Tintinnopsella longa*, *Lorenziella hungarica*, aptychy, bivalves, ostracods. Matrix contains dispersed pyrite, also part of the organic fragments is impregnated by Fe oxides. ***Elliptica* Subzone** of the ***Calpionella* Zone**.

No. 4.0
Radiolarian-calpionella wackestone, radiolarians, aptychy, bivalves, *Calpionella alpina*, *Tintinnopsella carpathica* and *Remaniella catalanoi*.

No. 3.8
Radiolarian-calpionella wackestone. Radiolarians, *Calpionella alpina*, *Calpionella elliptica*, *Tintinnopsella carpathica*, *Tintinnopsella longa*, *Schizosphaerella minutissima*, bivalves, aptychy and crinoids.

No. 3.6
Radiolarian-calpionella wackestone. Radiolarians, *Calpionella alpina*, *Calpionella elliptica*, *Tintinnopsella carpathica*, *Tintinnopsella longa*, *Remaniella catalanoi*, bivalves, aptychy and ostracods.

No. 3.4
Radiolarian-calpionella wackestone. Radiolarians, *Calpionella alpina*, *Calpionella elliptica*, *Tintinnopsella carpathica*, *Tintinnopsella longa*, *Remaniella catalanoi*, *Remaniella duranddelga* (part of loricas have dark coats), aptychy, bivalves and crinoids.

No. 3.2
Radiolarian-calpionella wackestone. Radiolarians, *Calpionella alpina*, *Calpionella elliptica*, *Tintinnopsella carpathica*, *Tintinnopsella longa*, *Remaniella duranddelgai*, *Remaniella catalanoi*. Abundant calcite veins oriented in several different directions.

No. 3.0
Radiolarian-calpionella wackestone. Fractures of several orientation filled by calcite. Radiolarians, bivalves, *Calpionella alpina*, *Tintinnopsella carpathica* and *Remaniella catalanoi*.

No. 2.8
Radiolarian-calpionella wackestone. Radiolarians, aptychy, bivalves, crinoids, *Calpionella alpina*, *Tintinnopsella carpathica* and calcite veins.

No. 2.8
Radiolarian-calpionella wackestone. Radiolarians, aptychy, bivalves, crinoids, *Calpionella alpina*, *Tintinnopsella carpathica* and calcite veins.

No. 2.6
Radiolarian-calpionella wackestone. Radiolarians, sponges, ostracods, *Calpionella alpina*, *Tintinnopsella carpathica*, *Remaniella catalanoi* and *Cadosina semiradiata fusca*.

No. 2.4
Radiolarian-calpionella wackestone. Radiolarians, ostracods, *Calpionella alpina*, *Tintinnopsella carpathica*, *Remaniella duranddelgai*. Calcite veins.

No. 2.2
Radiolarian-calpionella wackestone passing to mudstone. Aptychy, *Punctaptychus*, ostracods, (2 % of thin shells), radiolarians, bivalves, *Calpionella alpina*, *Tintinnopsella carpathica* and *Lorenziella hungarica*

No. 2.0
Radiolarian-calpionella wackestone passing to mudstone. Radiolarians, *Calpionella alpina*, *Calpionella elliptica*, *Tintinnopsella carpathica*, *Tintinnopsella longa*, *Cadosina semiradiata fusca*, bivalves and ostracods.

No. 1.8
Radiolarian-calpionella wackestone. Radiolarians, aptychy, bivalves, ostracods, *Calpionella alpina*, *Tintinnopsella carpathica*, *Remaniella catalanoi* and *Lorenziella hungarica*.

No. 1.6
Radiolarian-calpionella wackestone. Radiolarians, aptychy, bivalves, ostracods, *Calpionella alpina*, *Tintinnopsella carpathica*, *Remaniella duranddelgai*, *Remaniella catalanoi*.

No. 1.4
Radiolarian-calpionella wackestone. Radiolarians, aptychy, bivalves, ostracods, *Calpionella alpina*, *Tintinnopsella carpathica*, *Remaniella catalanoi* and *Lorenziella hungarica*.

No. 1.2
Radiolarian-calpionella wackestone. Radiolarians, aptychy, bivalves, ostracods, *Lenticulina* sp., *Calpionella alpina*, *Tintinnopsella carpathica* and *Cadosina semiradiata fusca*.

No. 1.0
Radiolarian-calpionella wackestone. Radiolarians, sponge spicules, aptychy, foraminifers, bivalves, *Calpionella alpina* and *Tintinnopsella carpathica*.

No. 0.8
Radiolarian-calpionella wackestone. Radiolarians, aptychy, bivalves, foraminifers, *Calpionella alpina*, *Calpionella elliptica*, *Tintinnopsella carpathica*, *Remaniella catalanoi* and *Cadosina semiradiata fusca*.

No. 0.6
Radiolarian-calpionella wackestone. Radiolarians, Aptychy, bivalves, *Calpionella alpina*, *Calpionella elliptica*, *Tintinnopsella carpathica*, *Remaniella duranddelgai*, *Remaniella catalanoi*, *Cadosina semiradiata fusca* and *Schizosphaerella minutissima*.

No. 0.4
Radiolarian-calpionella wackestone. Radiolarians, aptychy, bivalves, *Calpionella alpina*, *Calpionella elliptica*, *Tintinnopsella carpathica*, *Tintinnopsella longa*, *Remaniella catalanoi*, *Remaniella duranddelgai* and *Cadosina semiradiata fusca*.

No. 0.2
Radiolarian-calpionella wackestone – radiolarians, aptychy, bivalves, *Calpionella alpina*, *Remaniella catalanoi* and *Tintinnopsella carpathica*.

No. 0.0
Radiolarian-calpionella wackestone – radiolarians, *Calpionella alpina*, *Calpionella elliptica*, *Tintinnopsella carpathica* and *Cadosina semiradiata fusca*.

Plate 1

Fig. 1: *Carpistomiosphaera borzai* (NAGY) in bioturbated mudstone. Sample No. 17.2 (NHMW 2008z0271/0001).

Fig. 2: *Parastomiosphaera malmica* (BORZA) in bioturbated mudstone with rare skeletal debris. Sample No.13.0 (NHMW 2008z0271/0002).

Fig. 3: *Cadosina semiradiata semiradiata* WANNER in bioturbated mudstone with rare skeletal debris. Sample No. 17.0 (NHMW 2008z0271/0003).

Fig. 4: *Colomisphaera pulla* (BORZA) in biomicrite mudstone. Frequent skeletal fragments are concentrated in thin laminae. Sample No. 11.8 (NHMW 2008z0271/0004).

Figs 5-6: *Colomisphaera fortis* ŘEHÁNEK in bioturbated mudstone with rare skeletal debris dispersed in the micrite matrix. Sample No.10.8 (NHMW 2008z0271/0005).

Fig. 7: *Colomisphaera tenuis* (NAGY) in bioturbated mudstone containing rare skeletal debris dispersed in the micrite matrix. Sample No. 10.8 (NHMW 2008z0271/0005).

Figs 8-9: *Stomiosphaerina proxima* ŘEHÁNEK in radiolarian-calpionellid wackestone. Samples No. 9.4 (NHMW 2008z0271/0006) and No. 6.0 (NHMW 2008z0271/0007).

Scale bars equal 50 µm.

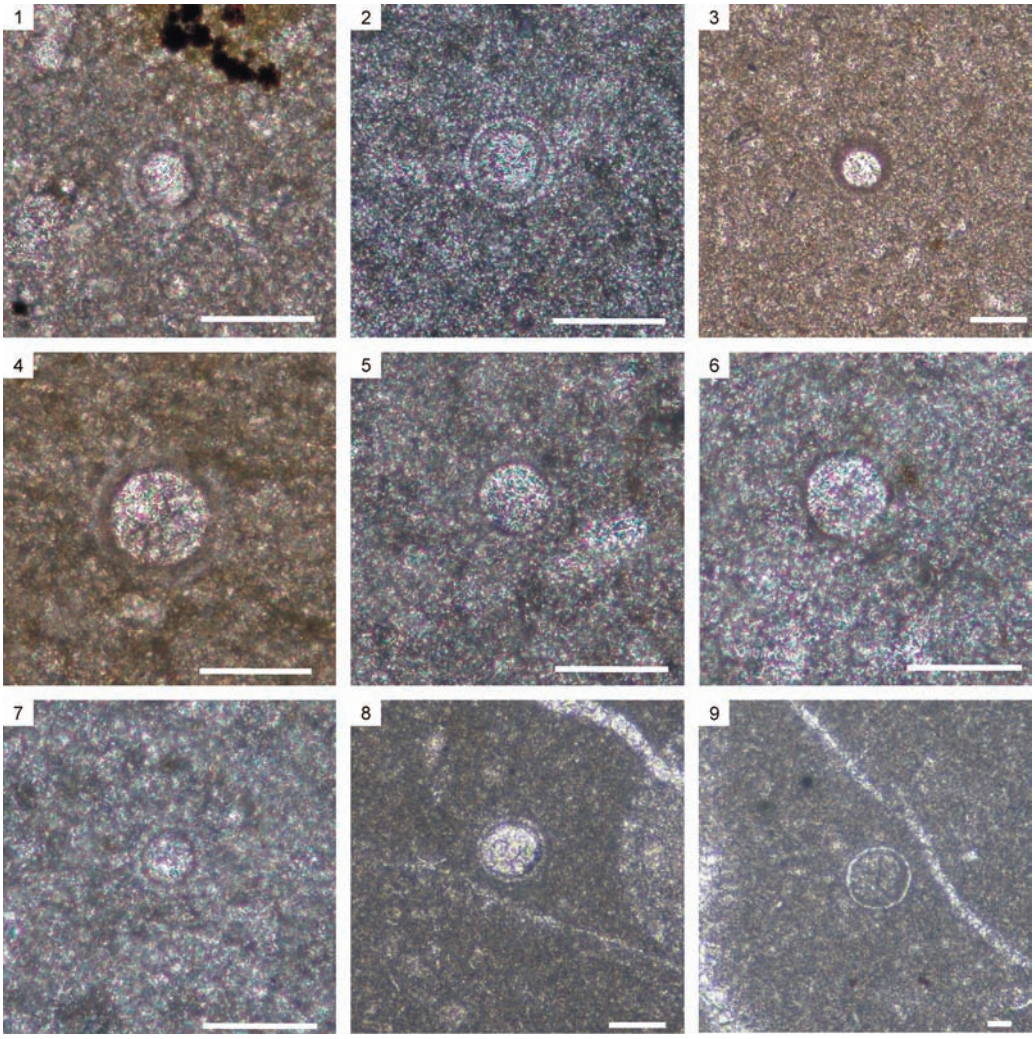
1
2
3
4
5
6
7
8
9

Plate 2

Fig. 1: *Borziella slovenica* (BORZA) in mudstone containing rare skeletal debris dispersed in the micrite matrix. Sample No. 11.0 (NHMW 2008z0271/0008).

Fig. 2: *Chitinoidella boneti* DOBEN in biomicrite limestone – mudstone with skeletal debris concentrated in thin laminae. Sample No. 11.6 (NHMW 2008z0271/0009).

Fig. 3: *Tintinnopsella remanei* BORZA in mudstone containing laminae of fine skeletal debris. Sample No. 10.1 (NHMW 2008z0271/0010).

Fig. 4: *Calpionella alpina* LORENZ and *Calpionella grandalpina* NAGY in radiolarian-calpionellid wackestone. Sample No. 9.8 (NHMW 2008z0271/0011).

Fig. 5: *Crassicollaria parvula* REMANE and *Calpionella grandalpina* NAGY in radiolarian-calpionellid wackestone. Sample No. 9.6 (NHMW 2008z0271/0012).

Fig. 6: *Remaniella duranddelgai* POP in calpionellid-radiolarian wackestone. Sample No. 4.4 (NHMW 2008z0271/0013).

Fig. 7: *Tintinnopsella longa* (COLOM) in radiolarian-calpionellid wackestone. Sample No. 3.4 (NHMW 2008z0271/0014).

Fig. 8: *Remaniella catalanoi* POP in radiolarian-calpionellid wackestone. Sample No. 3.4 (NHMW 2008z0271/0014).

Fig. 9: *Calpionella elliptica* CADISCH in radiolarian-calpionellid wackestone. Sample No. 3.2 (NHMW 2008z0271/0015).

Scale bars equal 50 µm.

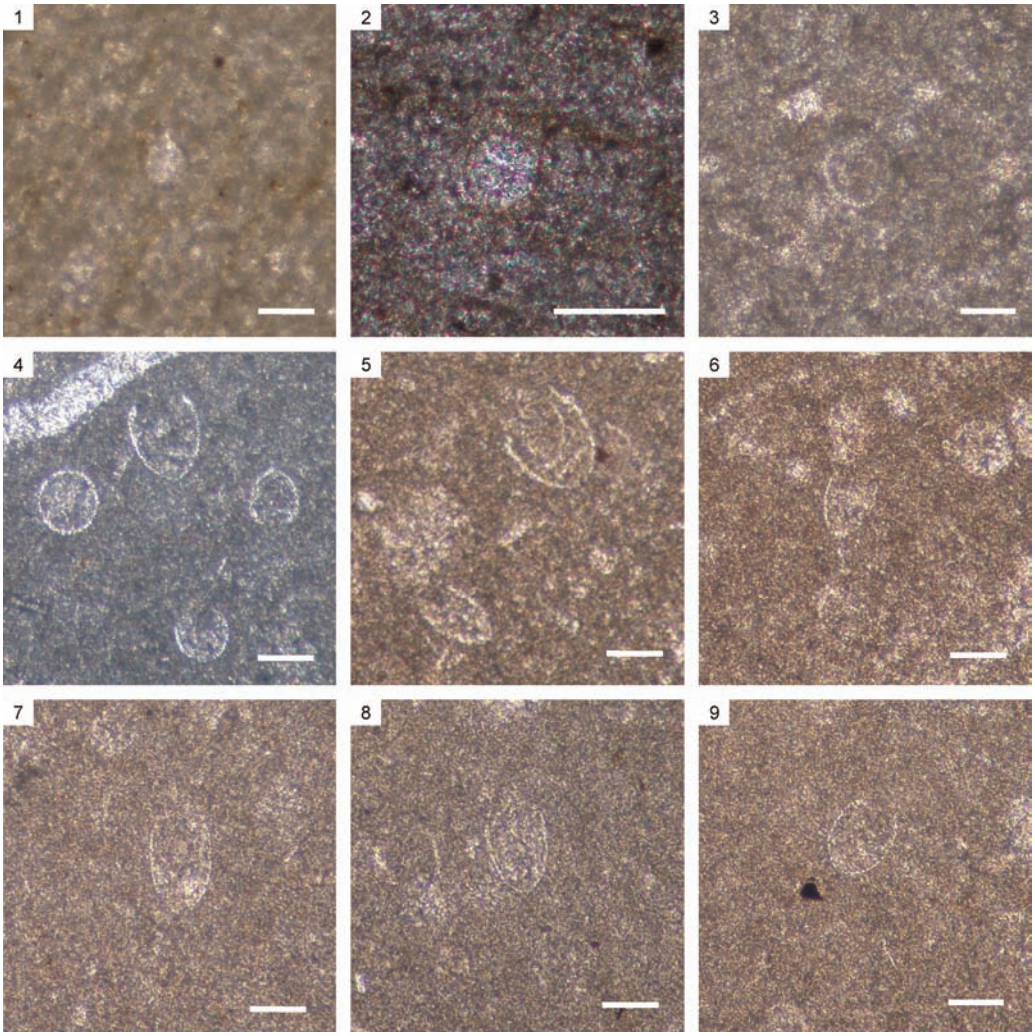
1
2
3
4
5
6
7
8
9

Plate 3

Fig. 1: Bioturbated biomicrite mudstone. Fine skeletal debris accumulated in circular swirl. Sample No. 15.8 (NHMW 2008z0271/0016).

Fig. 2: Fine skeletal fragments impregnated by Fe hydroxides concentrated in burrow filling. The absence of compaction indicates firmground substrate consistency. Sample No. 15.8 (NHMW 2008z0271/0016).

Fig. 3: Fine skeletal fragments and nests rich in Fe hydroxide accumulations. Sample No. 15.8 (NHMW 2008z0271/0016).

Fig. 4: Pyritized radiolarian tests in biomicrite mudstone. Sample No. 13.6 (NHMW 2008z0271/0017).

Fig. 5: Lamination due to parallel oriented fragments of *Saccocoma* sp. Sample No. 11.6 (NHMW 2008z0271/0009).

Fig. 6: Accumulation of pyrite cubes in biomicrite mudstone. Sample No. 11.4 (NHMW 2008z0271/0018).

Scale bars equal 100 µm.

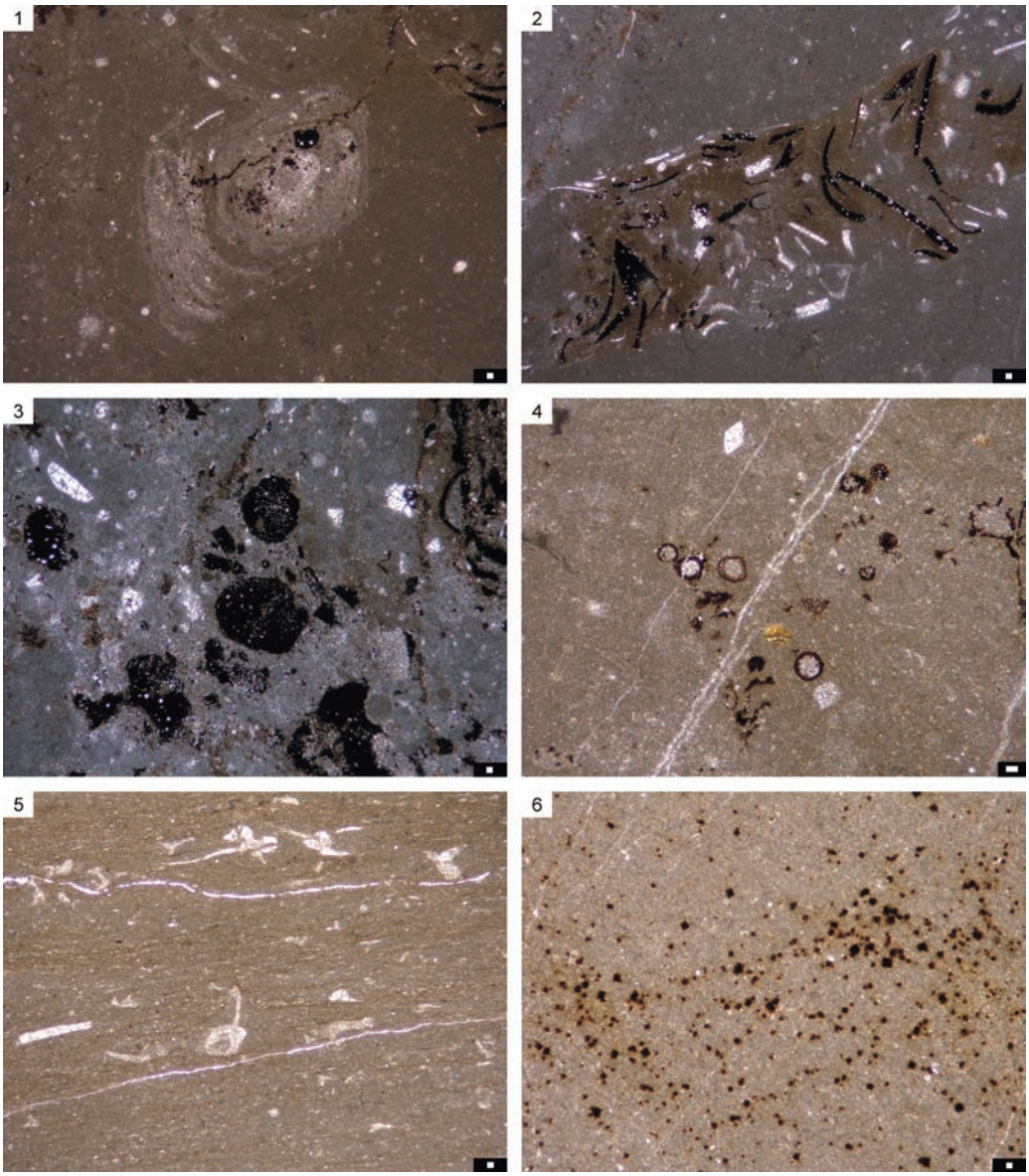
1
2
3
4
5
6

Plate 4

Fig. 1: Rhyncholite in biomicrite mudstone in marly biomicrite mudstone. Sample No.15.6 (NHMW 2008z0271/0019).

Fig. 2: Marks of synsedimentary deformation on the base of sample No. 12.2 (NHMW 2008z0271/0020).

Figs 3-4: Microsparitic laminae with peloids and *Cadosina semiradiata semiradiata* WANNER in biomicrite limestone – mudstone. Variously shaped micritic grains – mud peloids, commonly without internal structures. Grains originated from the reworking of weakly lithified carbonate mud; they were transported in suspension. Sample No. 10.6 (NHMW 2008z0271/0021).

Fig. 5: Radiolarian-calpionellid wackestone penetrated by thin calcite veins. Sample No. 9.8 (NHMW 2008z0271/0011).

Fig. 6: Biomicrite mudstone with *Calpionella alpina* LORENZ penetrated by calcite veins of various size and orientation. Sample No. 6.4 (NHMW 2008z0271/0022).

Scale bars equal 100 µm.

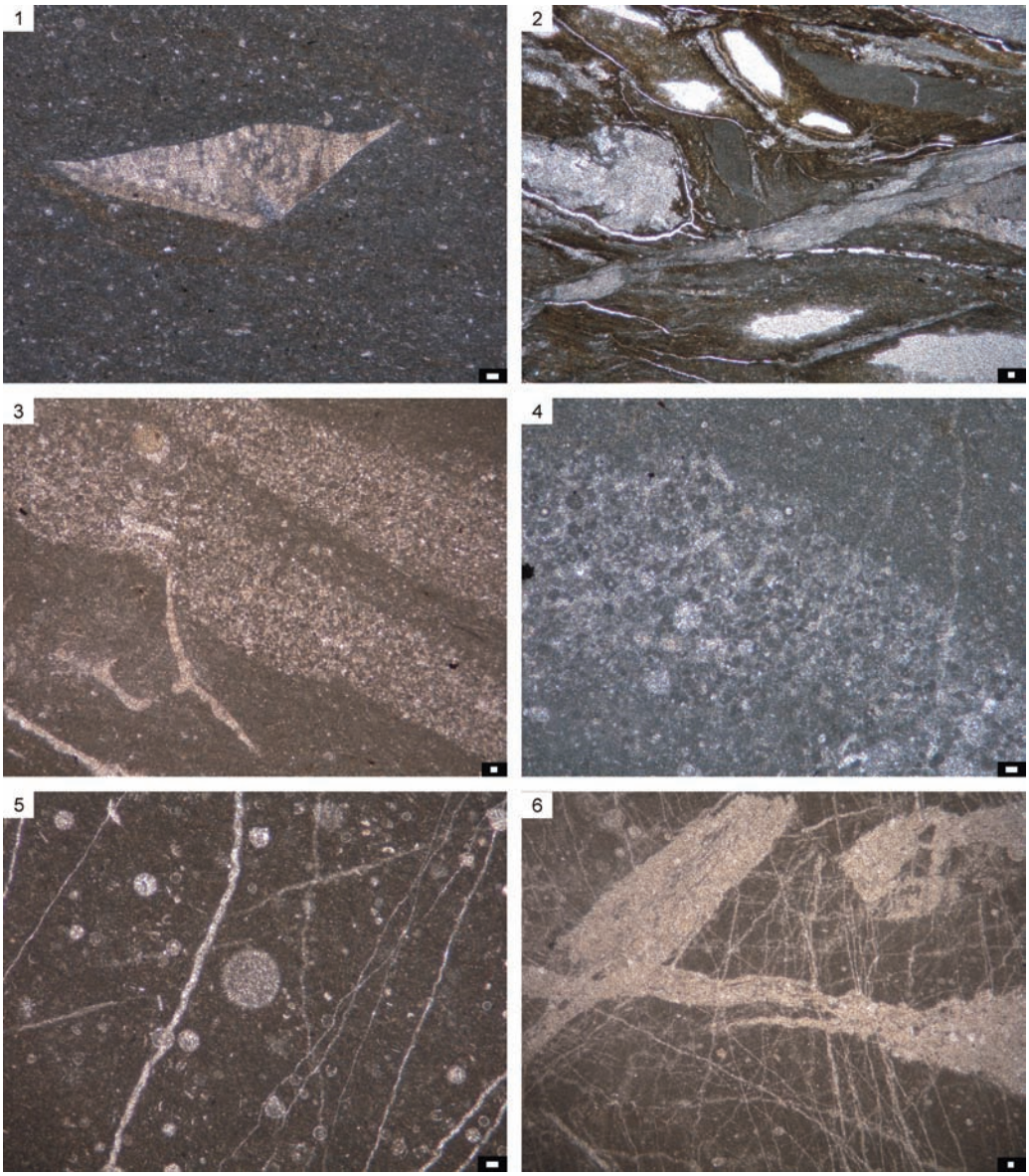
1
2
3
4
5
6

Plate 5

Fig. 1: *Zeugrhabdotus embergeri* (NOËL) PERCH-NIELSEN; Sample No. 15.0 (NHMW 2008z0271/0023).

Fig. 2: *Zeugrhabdotus erectus* (DEFLANDRE) REINHARDT; Sample No. 10.0 (NHMW 2008z0271/0024).

Fig. 3: *Discorhabdus ignotus* (GÓRKA) PERCH-NIELSEN; Sample No. 9.0 (NHMW 2008z0271/0025).

Fig. 4: *Helenea chiastia* WORSLEY; Sample No. 11.0 (NHMW 2008z0271/0008).

Fig. 5: *Speetonia colligata* BLACK; Sample No. 8.0 (NHMW 2008z0271/0026).

Figs 6-8: *Watznaueria barnesae* (BLACK) PERCH-NIELSEN; Samples No. 9.0 (NHMW 2008z0271/0025), 17.0 (NHMW 2008z0271/0003), 9.0 (NHMW 2008z0271/0025).

Fig. 9: *Watznaueria britannica* (STRADNER) REINHARDT; Sample No. 18.0 (NHMW 2008z0271/0028).

Fig. 10: *Watznaueria ovata* BUKRY; Sample No. 9.0 (NHMW 2008z0271/0025).

Figs 11-12: *Cyclagelosphaera margerelii* NOËL; Samples No. 18.0 (NHMW 2008z0271/0028), 15.0 (NHMW 2008z0271/0023).

Fig. 13: *Cyclagelosphaera deflandrei* (MANIVIT) ROTH; Sample No. 17.0 (NHMW 2008z0271/0003).

Fig. 14: *Diazomatholithus lehmannii* NOËL; Sample No. 3.0 (NHMW 2008z0271/0029).

Figs 15-18: *Conusphaera mexicana* TREJO subsp. *mexicana* BRALOWER et al.; Samples No. 11.0 (NHMW 2008z0271/0008), 15.0 (NHMW 2008z0271/0023), 17.0 (NHMW 2008z0271/0003).

Figs 19-20: *Conusphaera mexicana* Trejo subsp. *minor* BOWN & COOPER; Sample No. 18.0 (NHMW 2008z0271/0028).

Figs 21-22: *Faviconus multicolumnatus* BRALOWER in BRALOWER et al.; Samples No. 14.0 (NHMW 2008z0271/0030), 17.0 (NHMW 2008z0271/0003).

Figs 23-24: *Nannoconus compressus* BRALOWER & THIERSTEIN in BRALOWER et al.; Sample No. 11.0 (NHMW 2008z0271/0008).

Figs 25-26: ?*Nannoconus wintereri* BRALOWER & THIERSTEIN in BRALOWER et al.; Sample No. 9.0 (NHMW 2008z0271/0025).

Figs 27-28: *Nannoconus globulus* BRÖNNIMANN ssp. *minor* BRALOWER in BRALOWER et al.; Samples No. 7.0 (NHMW 2008z0271/0032), 5.0 (NHMW 2008z0271/0033).

Fig. 29: *Nannoconus cornuta* DERES & ACHÉRITÉQUY; Sample No. 5.0 (NHMW 2008z0271/0033).

Fig. 30: *Nannoconus steinmanni steinmanni* KAMPTNER; Sample No. 4.0 (NHMW 2008z0271/0034).

Light micrographs using an Olympus CAMEDIA digital camera C-4000 Zoom.
Scale bars equal 1 µm

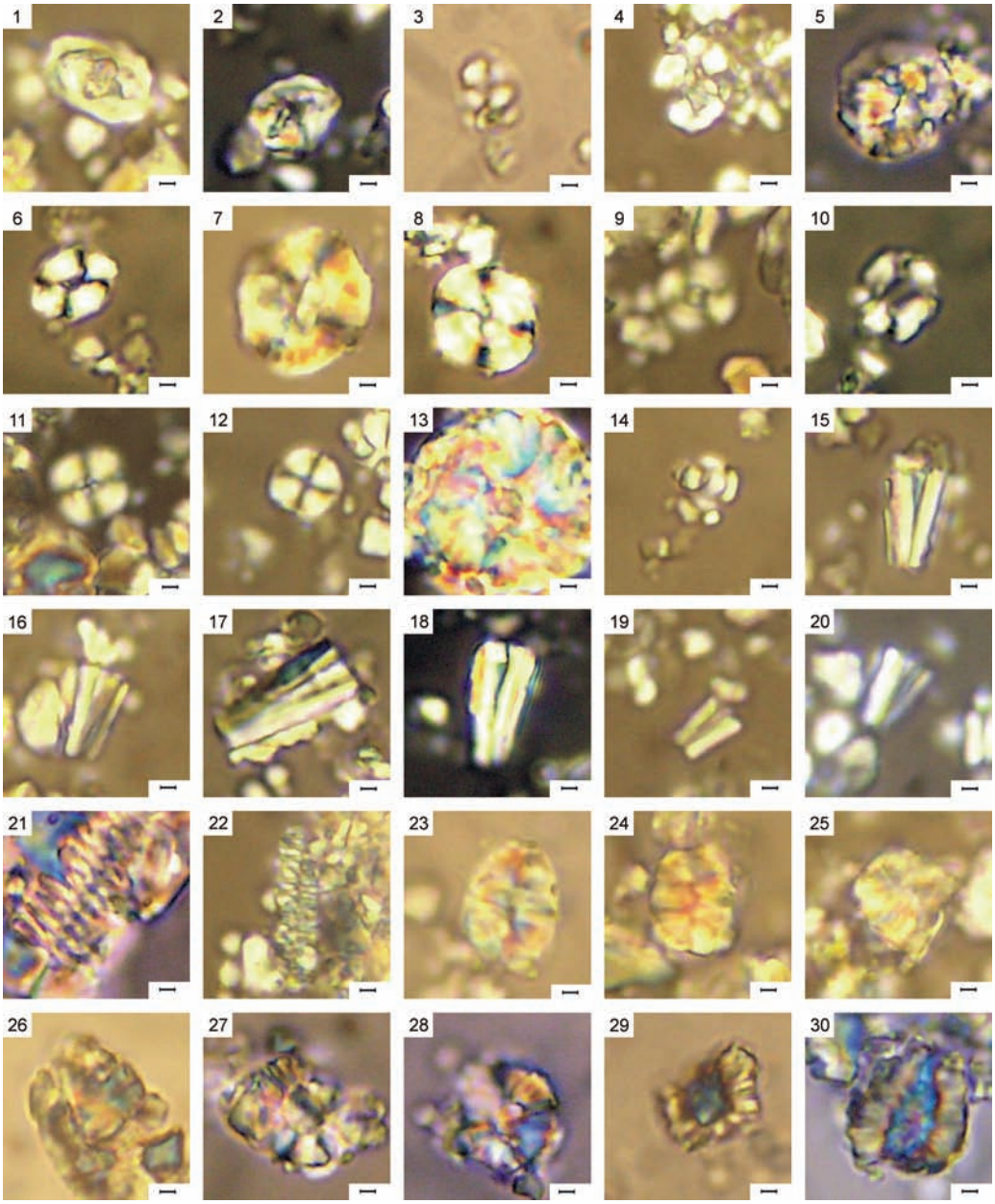
1
2
3
4
5
6
7
8
9
10
11
12
13
14
15
16
17
18
19
20
21
22
23
24
25
26
27
28
29
30

Plate 6

Fig. 1: *Nannoconus steinmanni minor* DERES & ACHÉRITÉQUY; Sample No. 4.0 (NHMW 2008z0271/0034).

Figs 2-3: *Nannoconus kamptneri kamptneri* BRÖNNIMANN; Sample No. 4.0 (NHMW 2008z0271/0034).

Figs 4, 8, 9: *Nannoconus steinmanni steinmanni* KAMPTNER; figs show the same specimen, Sample No. 3.0 (NHMW 2008z0271/0029).

Fig. 5: *Nannoconus globulus globulus* BRÖNNIMANN; Sample No. 3.0 (NHMW 2008z0271/0029).

Fig. 6: *Nannoconus kamptneri kamptneri* BRÖNNIMANN; Sample No. 3.0 (NHMW 2008z0271/0029).

Figs 7, 11: *Nannoconus globulus* Brönnimann ssp. *minor* BRALOWER in BRALOWER et al.; Samples No. 3.0 (NHMW 2008z0271/0029), 2.0 (NHMW 2008z0271/0035).

Fig. 10: *Nannoconus kamptneri minor* BRALOWER in BRALOWER et al.; Sample No. 3.0 (NHMW 2008z0271/0029).

Fig. 12: *Nannoconus* spp.; Sample No. 2.0 (NHMW 2008z0271/0035).

Fig. 13: *Nannoconus steinmanni minor* DERES & ACHÉRITÉQUY; Sample No. 2.0 (NHMW 2008z0271/0035).

Fig. 14: *Nannoconus kamptneri minor* BRALOWER in BRALOWER et al.; Sample No. 2.0 (NHMW 2008z0271/0035).

Fig. 15: *Nannoconus kamptneri kamptneri* BRÖNNIMANN; Sample No. 2.0 (NHMW 2008z0271/0035).

Figs 16-18: *Nannoconus steinmanni minor* DERES & ACHÉRITÉQUY; Sample No. 2.0 (NHMW 2008z0271/0035).

Figs 19-20: *Nannoconus steinmanni steinmanni* KAMPTNER; Sample No. 2.0 (NHMW 2008z0271/0035).

Figs 21-26: *Polycostella beckmannii* THIERSTEIN; Samples No. 16.0 (NHMW 2008z0271/0036), 14.0 (NHMW 2008z0271/0030), 13.0 (NHMW 2008z0271/0002).

Figs 27-28: *Assipetra infracretacea* (THIERSTEIN) ROTH; Samples No. 7.0 (NHMW 2008z0271/0032), 8.0 (NHMW 2008z0271/0026).

Figs 29-30: *Hexalithus noeliae* LOEBLICH & TAPPAN; Samples No. 7.0 (NHMW 2008z0271/0032), 11.0 (NHMW 2008z0271/0008).

Light micrographs using Olympus CAMEDIA digital camera C-4000 Zoom.
Scale bars equal 1 µm.

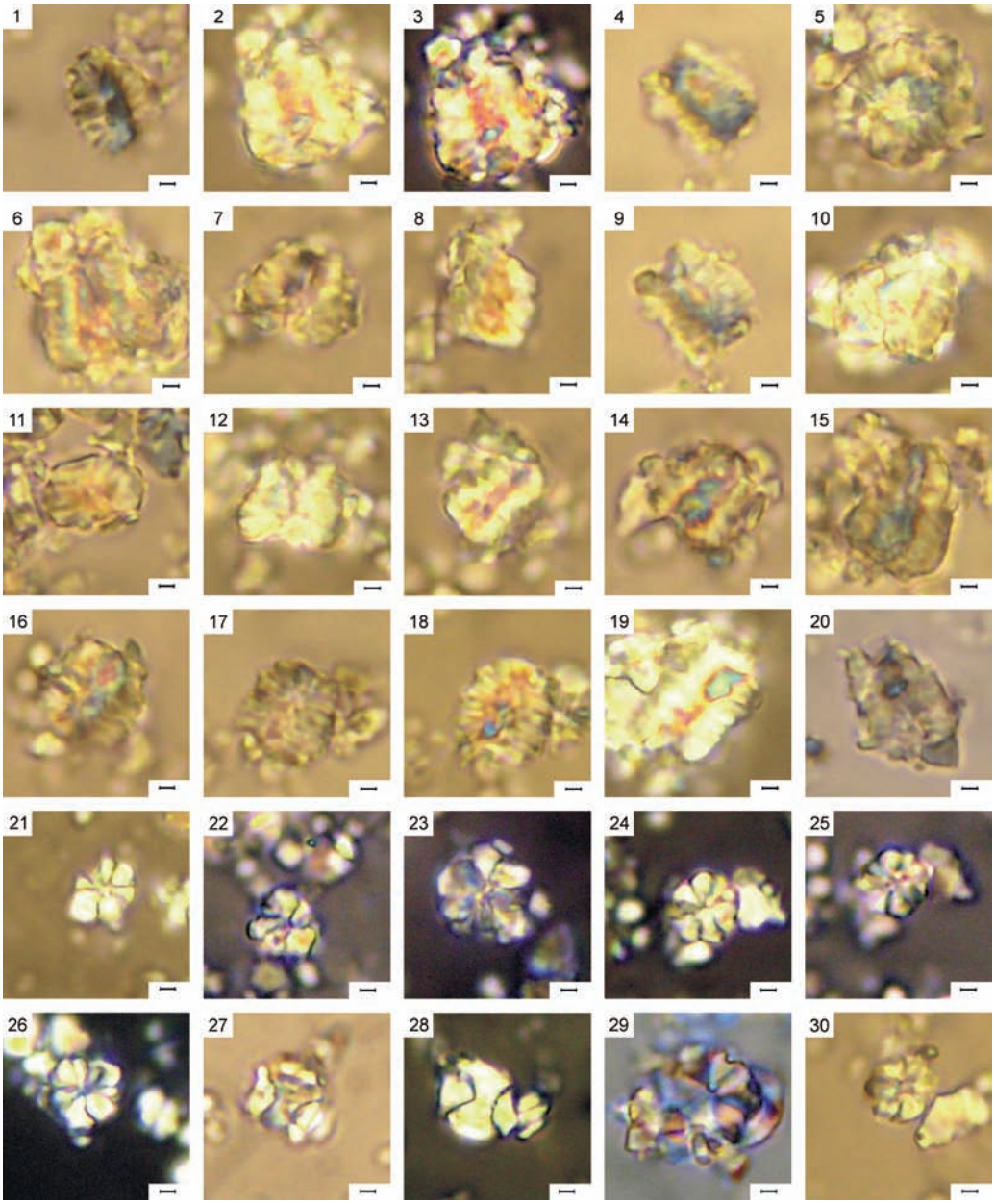
1
2
3
4
5
6
7
8
9
10
11
12
13
14
15
16
17
18
19
20
21
22
23
24
25
26
27
28
29
30